Basement-cover tectonics, structural inheritance and deformation migration in the outer parts of orogenic belts: A view from the western Alps

Robert W.H. Butler

Geology and Petroleum Geology, School of Geosciences, University of Aberdeen, Aberdeen AB24 3UE, Scotland, Britain.

ABSTRACT

The structure and geology of former rifted continental margins can exert significant influence on their subsequent incorporation into collisional orogens. While thinned continental crust attached to the subducting mantle lithosphere may be incorporated into subduction channels, the weakly rifted parts of the margin are likely to resist subduction and thus deform ahead of the main orogenic front. This expectation is corroborated by a case study from the external western Alps. The former Dauphinois basins have inverted to form external basement massifs. Much of the deformation was widely distributed, with few localised thrust structures. Existing models that invoke distinct deformation events, separated in time by a major (late Eocene, "Nummulitic") unconformity are abandoned here in favour of crustal shortening that was continuous in time. Integrated stratigraphic, paleothermal and geochronological data reveal that basin inversion was protracted over 6-10 Myr, coeval with deformation in the more internal parts of the chain. The notion of continuous, rather than episodic, deformation raises issues for how rates and tectonic activity may be evaluated within ancient orogens.

Keywords: tectonic inversion, Alps, foredeep, basement deformation

INTRODUCTION

There is a tacit assumption in tectonic models of mountain belts that deformation simply steps out into the foreland with time. But such assumptions are also implicit in many orogenic reconstructions and in strategies adopted for balancing and restoring regional cross-sections. Indeed structures that may not conform to this assumption are generally referred to as being "out-of-sequence", reinforcing the notion that simple forelandward migration is the norm. The aim of this paper is to discuss the issue of the migration of deformation in mountain belts and how it has been influenced by pre-existing structures.

Large-scale structural inheritance and its impact on the patterns of crustal shortening are inferred for many orogens (Appalachians, e.g., Hatcher and Hooper, 1992; Papua New Guinea, e.g., Hill and Hall, 2002; Pyrenees, e.g. Roure et al., 1989). However, in many cases the basement regions have been exhumed from the once deeply-buried internal parts of mountain belts (e.g. McBride et al., 2005) so that erosion has removed much of the key evidence for inherited basin faults. The Alps are a rare example where critical geological relationships are preserved, not least because the former rifted continental margin that existed prior to deformation was highly sediment-starved (e.g. Lemoine et al., 1986). They may therefore inform the interpretation and future investigation of other orogens.

The external western Alps provide the case study. The region has seen a number of contrasting interpretations of basement-cover tectonics that have different implications for crustal structure. These are reviewed and a preferred model is then integrated with a variety of existing paleothermal and geochronological data, together with important stratigraphic relationships. This in turn informs a discussion of deformation migration within the western Alps. Many of these relationships are well-known in the existing literature but are generally viewed as resulting from pulsed tectonics that operated in distinct episodes. The aim here is to show that the geological relationships are better understood in terms of a continuum. Protracted deformation that is heterogeneously distributed both in space and time is an expectation of orogenic evolution of former rifted continental margins with their inherent heterogeneity in lithosphere structure. This re-evaluation raises issues of how the evolution of

orogenic belts can be resolved, especially when syn-tectonic sedimentation is no longer preserved.

It is increasingly recognised that simple thrust evolution is strongly controlled by the presence of pre-existing structures (Butler et al., 2006, and references therein). These can act to localise thrusts or influence their trajectories. Most studies assume that these inherited structures simply influence the detail of local thrust trajectories rather than necessarily controlling the overall development of the orogen. However, recent advances in understanding the structure of rifted continental margins emphasise the presence of heterogeneities beyond simple rift faults that could exert more fundamental influences on orogenic structure (e.g. Péron-Pinvidic and Manatschal, 2010, and references therein). These include abrupt changes in crustal thickness and large-scale tracts of serpentinized upper mantle that could influence coupling between crust and mantle in evolving orogens. Two recent studies explore the significance of these heterogeneities.

Butler et al. (2013) show from modelling that large-scale rifted margin structure can exert a first-order control on how the continental crust deforms within a convergent system. Previously thinned crust can be subducted, recording this burial through the acquisition of ultra-high-pressure metamorphic mineral assemblages. Return of these deeply buried segments of crust requires their decoupling from the otherwise subducting plate (Fig. 1). In contrast, the weakly rifted landward components of the rifted margin resist subduction and thicken at the top of the subduction channel, while the subduction of the previously thinned crust can continue. The deformation of the continental crust at the mouth of the subduction channel can continue over a protracted time. Butler (2013) notes that the original coupling between crust and mantle that has been inherited from the rifting phase will limit these behaviours (Fig. 1). This coupling is likely to vary, perhaps reflecting differing amounts of water ingress into the upper mantle and its associated serpentinization, during the later stages of rifting (e.g., Péron-Pinvidic and Manatschal, 2010).

In the western Alps, the focus of this study, it is the external zones and their basement massifs that represent the weakly rifted parts of the former continental margin (e.g. Lemoine et al., 1986; Mohn et al., 2010). While rift

structures and their influence on Alpine compressional tectonics have long been recognised (e.g. Gillcrist et al., 1987; Butler, 1989; Dumont et al., 2008; Bellahsen et al., 2012; Butler, 2013), the significance of protracted deformation is less well-established. Many other orogens have similarly developed by contractional deformation acting upon pre-existing basin systems and other forms of inherited structures that collectively represent significant lateral heterogeneities in continental crustal structure. Thus, although the focus in this paper is on an Alpine case study, it is likely that the deductions reached here are relevant to many other orogenic systems.

ALPINE CONTEXT

The western Alps are a classic example of a basement-cover thrust system, derived from stacked portions of the former European margin of the Tethyan ocean system. The chain has developed between the Apulian continental block (essentially the Italian peninsular and Adriatic region) and the rest of Europe. The outer parts of the mountain belt, the focus of this paper, are found in SE France.

Pre-orogenic basement and cover units

The regional geological and stratigraphic context for the western Alps is widely described (see de Graciansky et al., 2013 for a readable account). Basement rocks of the foreland outcrop in the French Massif Central where they record a complex history of metamorphism, magmatism and deformation. This culminated with the Variscan orogeny that deformed most of what is now western and central Europe during the late Paleozoic (e.g. Schulmann et al., 2014, and references therein). This heterogeneous crust is incorporated into the Alps and is exposed in the so-called “external basement massifs” (e.g. Raumer et al., 2009; Fig. 2).

The external Alpine basement is overlain unconformably by a Mesozoic cover succession. This begins with a thin (<50m) Triassic sequence chiefly comprising shallow-marine quartz sandstones, dolostones and local evaporites

that chart both planation of the pre-existing Variscan chain and marine transgression. The overlying Jurassic and Lower Cretaceous strata chart heterogeneous subsidence across the region – with modern accounts stressing the importance of early Jurassic rifting followed by a protracted phase of post-rift thermal subsidence. This period is characterised by limestone and shale deposition, with virtually no siliciclastic input. A series of carbonate platforms are widely interpreted to have built out from less rifted Europe (represented now by central France) towards the fledgling Tethyan ocean. In the NW Alps, the most recent of these platforms forms a lithostratigraphic unit termed the "Urgonian", of Hauterivian-Barremian (Early Cretaceous) age. The maximum extent of the carbonate platforms is well constrained by a few spectacular outcrops (Clavel et al., 2013) within the Subalpine chains. Oceanward of the platforms, sedimentation rates are inferred to decrease so that, across much of the region, the Mesozoic rift basins were under-filled. In the SW Alps, platform carbonates that built out from Provence (Fig. 2) continued into the Late Cretaceous. Thick basinal sediments accumulated, essentially keeping pace with subsidence to accumulate over 9 km of Mesozoic strata in the Vocontian Basin (e.g. de Graciansky et al., 2013, and references therein; Fig. 2). Thus not all the continental margin was starved of platform-derived sedimentation, as implied in some syntheses (e.g. Lemoine et al., 1986).

Contractional deformation in SE France, that culminated in the formation of the Alps, is generally viewed as having had a long and complex history. Much significance is placed on an angular unconformity in the Dévoluy area (Gidon et al., 1970; Fig. 2) that truncates folded strata up to Early Cretaceous in age and is overlain by Upper Cretaceous pelagic limestones. The tectonic status of this deformation, demonstrably of Cretaceous age, is controversial. Although classically ascribed to "Pyrenean" tectonics and the initial convergence between Iberia and France, Dumont et al. (2011) consider them to be large-scale slump structures. Cretaceous deformation has also been proposed on the flanks of what is now the Ecrins basement massif (Fig. 2), although stratigraphic considerations here only indicate that deformation pre-dated late Priabonian (Late Eocene) times. Further discussion of the timing and significance of these ages of deformation is reserved until later.

The main Alpine deformation in SE France dates from the Eocene to earliest Pliocene (e.g. Dumont et al., 2011, and references therein). The onset is marked by a transgressive sequence of deposits generally ascribed to the fledgling Alpine foredeep and termed the "Nummulitic" (reviewed by Joseph and Lomas, 2004). It classically comprises three formations: a basal shallow water (Nummulitic) limestone; blue marls (the "Marnes Bleues") and a sequence of turbiditic sandstones that include the much-studied "Grès d'Annot" (Annot Sandstone). These lithostratigraphic units are diachronous, charting the lateral migration of the ancestral foredeep basin foreland-ward from the Lutetian to Priabonian (Mid-Late Eocene) (e.g. Sinclair, 1997; Ford and Lickorish, 2004; Dumont et al., 2011). Deposition is terminated by an olistostromal unit (the "Schistes a blocs") and the arrival of thrust sheets. Deformation continued through to the Pliocene , the age of strata in the footwall to the Digne thrust (Fig. 2). However, in the NW Subalpine chains it is likely that thrusting terminated in latest Miocene times (e.g. Dumont et al., 2011).

Subalpine chains

The external NW Alps can be divided into two distinct domains: The outer thrust belt of the Subalpine Chains; and the basement –involved structures of the Dauphinois. The Subalpine Chains are generally considered to be a "thin-skinned" fold and thrust belt detached on either thin Triassic evaporites or Jurassic shales (Gratier et al., 1989). Deformation incorporates syn-orogenic sandstones – with thrusts over-riding these Miocene strata in the Grenoble area (Fig. 2). These structures were broadly WNW-directed (Butler, 1992).

The Mesozoic stratigraphy changes markedly across the Subalpine fold-thrust belt. In the foreland-ward side the strata are chiefly platform carbonates and reach a thickness of no more than 2 km. In the east the stratigraphy expands to a thickness of around 6 km, and lies in more basinal facies (reviewed by de Graciansky et al., 2011). These variations chart the transition from the stable European continent towards the more rifted regions on the margins of the former Tethys ocean.

Most probably, thrust detachment under the Subalpine Chains roots beneath the westernmost basement units of the Alps – the Belledonne massif (Figs. 2 and 3; e.g. Butler et al., 1986; Gratier et al., 1989). This interpretation is consistent with deep seismic reflection profiling (Bayer et al., 1987) and is a general component of modern sections through the region (e.g. Schmid and Kissling, 2000; Schmid et al., 2004; Butler, 2013; Bellahsen et al., 2014). This Basal Belledonne Thrust was presumably responsible for the main uplift of the Dauphinois region that lies in its hanging wall. Sustained exhumation of the Dauphinois domain has been identified through inverse modelling of data from diverse thermochronological systems and dated at 13Ma – 8Ma (van der Beek et al., 2010). This Miocene age-range is consistent with the inferred coeval relationship between displacements on the Basal Belledonne Thrust and the emergent Subalpine Thrust system.

Dauphinois basement-cover system

While the Subalpine fold-thrust belt is dominated by outcrops of Cretaceous strata, especially of prograding carbonate platforms, the Dauphinois region to the east is characterised by outcrops of basement rocks, overlain locally by a few metres of Triassic shallow-water quartz sandstones and dolostones (with local basaltic lavas), together with basinal Jurassic shales. Over the past 50 years there have been competing structural interpretations of the relationship between crystalline basement and the Jurassic sedimentary cover. Early ideas considered the cover to lie within "pinched-in" synclines whose geometry simply reflected rheological variations (e.g. Ramsay, 1963; Fig. 4a). With the popularisation of thrust tectonic models, Beach (1981) interpreted the juxtaposition of basement and cover as the result of westward-directed thrust imbrication (Fig. 4b). He went on to interpret the northward limit of the Ecrins to be the result of lateral ramps, with crustal-scale imbricates cutting up-section to the north. This model was subsequently followed by Butler et al. (1986) in their regional study of Alpine thrusting. However, consideration of stratigraphic relationships within the Jurassic rocks and the recognition of Jurassic-age normal faults (Barféty et al., 1979) established that many of the cover slices in the Ecrins were compressed

half-graben. Thrusting, although important further east in the Ecrins, was generally abandoned as an explanation of basement-cover contacts for much of the massif (Gillcrist et al., 1987, Coward et al., 1991; Fig. 4c). Since then it has generally been assumed that the cover and basement of the Ecrins have shortened together, with limited detachment between them (e.g. Butler et al., 2006; Dumont et al., 2008; Fig. 4d). In these approximations, deformation is considered to involve heterogeneous sub-horizontal shortening. Since then Bellahsen et al., (2014) have argued for more localised simple-shear zones cutting the basement and then distributing the deformation upwards into the Jurassic cover (Fig. 4e).

Normal faults are increasingly being invoked within the pre-orogenic templates for orogenic belts (e.g. Butler et al., 2006). In the Dauphinois area many of the pre-orogenic faults preserve normal-sense (rift-related) throws (e.g. Dumont et al., 2008). However, it is not established whether some of the rift-related throw has been recovered by contractional reactivation of these faults during Alpine orogenesis. Most workers have long assumed that, because these faults preserve a net normal throw, they have not reactivated as thrusts – but this is an arbitrary assumption. Nevertheless, there is certainly significant basement deformation distributed away from these pre-existing faults (Dumont et al., 2008; Bellanger et al., 2015). This implies that the faults were not significantly weaker – either because of their frictional state or their orientation – than the host crystalline basement (Butler et al., 2006). Distributed basement weakening is consistent with mineralogical studies of the external Alpine basement. Former feldspars within granitic components in the basement have been altered to sericite suggesting significant hydrothermal alteration either before or during Alpine deformation (Wibberley, 1997; Francois and Lemet, 1999).

Despite significant Alpine deformation, some of the Mesozoic rift structures are famously well-preserved, with stratigraphic relationships interpreted as recording syn-rift deposition (Barféty et al., 1979). The best of these is the Ornon fault (Fig. 5a). This east-dipping structure serves as the eastern limit to the Taillefer massif (Fig. 3). Jurassic sediments in the hanging wall to the fault (Fig. 5b) are strongly deformed by upright folds and steeply-

263 dipping cleavage that is attributed to Alpine contraction buttressed against the
264 Jurassic fault block (e.g. Barféty et al., 1979). These geometries are similar to the
265 'mushwad' deformations within Cambrian shales deformed against basement
266 faults in the Appalachian thrust belt (e.g. Pashin et al., 2012). Basement in the
267 hanging wall to the Ornon fault forms the composite Grandes Rousses – Rochail
268 block (Fig. 4d). This block bounded to its east by the Mizoen fault that in turn has
269 the Emparis basement block in its hangingwall. Further eastwards the effects of
270 Alpine deformation become more pronounced so that the former presence of
271 Jurassic half-graben becomes more conjectural. The Meije block has been carried
272 by its eponymous thrust (Fig. 5c) to lie structurally above the Emparis block
273 (Plateau d'Emparis on Fig. 4d). Likewise, the Combeynot block has been
274 juxtaposed to structurally overlie the Meije (Fig. 5c).
275 The Combeynot basement block is statigraphically overlain by the
276 Nummulitic strata, with the local omission of the entire Mesozoic succession.
277 These turbidites (locally termed the Aiguilles d'Arves Sandstone) are tectonically
278 overlain by more internal Alpine units of the so-called Sub-Brianconnais domain.
279 The contact is generally considered to be one of the fundamental structures of
280 the Western Alps, termed the Frontal Pennine Thrust. Note however that some
281 compilations consider the Combeynot basement and its Tertiary cover to also lie
282 in the hanging wall to the Frontal Pennine Thrust (e.g. Schmid et al., 2004) – an
283 interpretation that will be revisited later.
284 Notwithstanding general understanding of the regional Alpine structure
285 of the Ecrins, there has been long-standing disagreement as to the timing and
286 significance of these structures. The key stratigraphic marker for these
287 deliberations has been the unconformity beneath the Nummulitic limestone and
288 its overlying foredeep turbidites. For some researchers (e.g. Beach, 1981),
289 basement thrusting and the formation of the Ecrins was exclusively "post
290 Nummulitic". Other researchers have emphasised the importance of pre-
291 Nummulitic deformation. In recent times this complex history has been
292 interpreted as distinct tectonic phases, one pre-Nummulitic and another post-
293 dating the youngest turbidites, which were deposited during the Oligocene (e.g.
294 Dumont et al., 2011). These relationships are central to the theme of this paper
295 and further discussion is reserved for later.

A SECTION THROUGH THE EXTERNAL FRENCH ALPS

A composite cross-section is presented here (Fig. 6) on the east-west transect across the external French Alps, passing close to the city of Grenoble (Fig. 2). The western part of this section illustrates the structure of the Vercors segment of the Subalpine chains (after Butler, 1987). Outcrop across the Vercors is dominated by the gently folded Urgonian platform carbonates. The frontal thrusts are shown with rather small displacements (c.f. Deville and Sassi, 2006) as they show en echelon map patterns and lateral tips just a few kms. out of the plane of section (Butler, 1987). Likewise thrusts within the Vercors show little displacement – the total shortening implied by the cross-section is around 8 km (Butler, 1987). This figure is significantly lower than equivalent sections further north along the Subalpine chains (Gratier et al., 1989; Butler, 1992), yet all these structures appear to root beneath the Basal Belledonne thrust. It is likely that this major thrust retained much of its displacement along strike – as the uplift of the basement rocks (the Belledonne massif) is sustained laterally. Butler (1987) proposed that the Vercors transect contains further shortening than is recorded in the broadly WNW-directed thrusts and that this segment of the Subalpine chains has also been partly backthrust over the leading edge of the Belledonne massif. These interpretations are also followed by Bellahsen et al. (2014). A total displacement on the Basal Belledonne Thrust, as accommodated within the Vercors fore-thrust – backthrust system, is estimated as 18 km.

The structure of the Dauphinois region is illustrated on Fig. 6 using the Romanche valley transect that runs between Bourg d'Oisans and La Grave (Fig. 3). Earlier interpretations of this specific section are shown on Fig. 4d,e. This profile has seen significant attention in recent years. Bellahsen et al. (2012) restored a section along this transect using the Triassic as a marker against which the underlying basement was reconstructed. Unlike much earlier attempts that used this method (e.g. Butler, 1986), these authors incorporated the concept that this Triassic marker was offset by pre-orogenic rift faults. Consequently their restored section shows the Ecrins in its pre-orogenic state containing an array of half-graben bounded by east-dipping normal faults. In this way the

329 restored section length across the Ecrins consists of the sum of the Triassic bed-
330 lengths together with all the heaves on the pre-orogenic normal faults. These
331 heave values are arbitrary because the original dip of the Jurassic structures is
332 uncertain.
333 Boutoux et al. (2014) present a revision of the Bellahsen et al. (2012)
334 restoration, based on integrated strain analyses in the strongly deformed lower
335 Jurassic cover sediments that represent the original fill to the various half-
336 graben. Comparison between the two restorations is difficult using percentage
337 shortening as they use different reference points. However, the effective
338 horizontal shortening may be compared. Boutoux et al's (2014) strain-based
339 restoration yields a shortening estimate of 8 km across the composite Ornon and
340 Mizoen half-graben. In contrast, Bellahsen et al's (2012) restoration using the
341 Triassic layer yields a shortening value of 9.7 km across the same half-graben.
342 While strain studies are useful for restoring the distributed contractional
343 deformation within the Jurassic half-graben, they do not address displacements
344 on discrete fault structures. It is unclear if the Jurassic normal faults have
345 themselves been reactivated. The section also contains two major thrusts that
346 carry the Combeynot and La Meije basement units. Direct determination of their
347 displacements from matching footwall and hanging-wall cut-offs is not possible.
348 Most interpretations (e.g. Fig. 4) indicate total displacements across these
349 thrusts in excess of 10km.
350
351 **Balancing the crust**
352
353 The structural geology exposed along the Romanche transect can now be
354 incorporated into a crustal scale section with the aim of establishing large-scale
355 shortening patterns in the outer parts of the western Alps. The workflows laid
356 out by Butler (2013) are followed here. For these purposes the top of the
357 basement on the transect is taken from the regional cross-section (Fig. 7). The
358 depth to the Moho across the Ecrins is taken from existing maps of crustal
359 thickness for the western Alps (Cavazza et al., 2004). It increases from around 30
360 km beneath the foreland to about 45 km beneath the Frontal Pennine Thrust and
361 the eastern Ecrins. Recent receiver function seismic modelling reported by Zhao

et al. (2015) also shows a gradual increase in crustal thickness beneath the Alps from the foreland. However, this experiment was located on a profile that runs across the inverted Vocontian basin rather than Ecrins. Thus it generally shows lower values for crustal thickness compared to those used here for the Ecrins section (Fig. 7).

The uncertainty on Moho depth on Fig. 7 is likely to be about 1-2km across the section as a whole. As the section is 120 km across, this equates to an uncertainty in estimates of crustal area of 100-200 km^2. In contrast, graphical measuring errors for crustal area are estimated at about 50 km^2. For the following construction a pin-line is established in the foreland of Bas Dauphine. The positioning of this pin is arbitrary, therefore percentage shortening values will not be reported for the cross-section as a whole. Rather, shortening is reported in parameterised km.

The total area of crust shown on the cross-section (Fig. 7) from a pin line in the Alpine foreland to a trail line beneath the Guisane valley (Frontal Pennine Thrust) is 4178 km^2. Using the inferred shortening in the Vercors system (18 km) as a proxy for displacement on the Basal Belledonne Thrust, the foreland crust has a top-basement length of 65 km from the pin line. This frontal portion, ahead of the footwall ramp to the Basal Belledonne Thrust, is considered to have not experienced significant distortional strain so it retains its lengths of top-basement and Moho. This distance of 65 km overlies a cross-sectional area of crust of 1717 km^2. The average thickness of this foreland crust is therefore 26.4 km. Assuming a pre-rifting (Triassic) depth to Moho of 30 km and uniform stretching (Jurassic), the crustal stretching factor is (30/26.4) = 1.14.

The remaining (4178-1717) 2461 km^2 of crust on the Ecrins transect (Fig. 7) represents the material that underlies the shortened Jurassic basins now found across the Ecrins massif. The present width of this basement, from an intermediate reference line at the leading edge of La Mure massif to the trail line in the Guisane valley, is 74 km. Bellahsen et al. (2012, 2014, modified by Boutoux et al., 2014) estimate that the net shortening of the top basement along this transect is 22 km. This yields a restored length of top basement of (74 +22) 96 km and an average restored thickness for the sub-Ecrins crust of (2461/96) 25.5 km.

The shortening estimates used above are conservative and probably underestimate displacements on Alpine thrusts. Additionally, they do not consider any contractional reactivation along the Jurassic normal faults. Allowing for these additional factors, the restored width of the former Dauphinois basins illustrated in Figure 7 is 110 km, with an implicit shortening of 36 km. Using the cross-sectional area of 2461 km^2, the mean restored crustal thickness beneath the Dauphinois basin can be estimated at (2461/110) = 22.4 km. This equates to a mean crustal stretching factor of 1.34 for uniform extension.

PALEOTHERMAL AND GEOCHRONOLOGICAL CONSTRAINS ON ECRINS DEFORMATION

The following account relies heavily on the recent comprehensive study by Bellanger et al. (2015), although the interpretations offered here differ from these authors. They present a suite of estimates for peak temperatures, using Raman spectroscopy applied to carbonaceous material sampled from Jurassic and Tertiary strata around the Ecrins. A subset of these data are displayed on Fig. 6. The highest peak temperatures (338°C) are recorded by the Jurassic strata of the Dauphinois basins. To the east of the Ornon fault, peak temperatures experienced by Jurassic rocks range between 319°C and 338°C. It is tempting to relate this thermal pattern to Alpine shortening (Bellanger et al., 2015).

Peak temperature data are also available for the eastern Subalpine domain, from Cretaceous strata adjacent to the Vercors plateau down into lower Jurassic strata in the Drac valley (Fig. 6; Bellanger et al., 2015). These display a systematic cooling, with the deepest strata recording peak temperatures of 329 °C. This peak value is consistent with estimates of deep burial during Mesozoic basin filling (Butler 1987; Bellahsen et al., 2012) together with relatively steep geothermal gradients (40°C /km; Phillippe et al., 1998) derived from high heat production in underlying basement (Deville and Sassi, 2006).

Elevated geotherms and high burial temperatures are also supported by peak temperature data from the Jurassic cover of the Dome de la Mure (Fig. 6). Bellanger et al. (2015) report peak temperatures here of 279°C. These strata lay

on a Jurassic fault block (e.g. de Graciansky et al., 2011). Adjacent, age-equivalent strata from the former basin areas record peak temperatures of 329°C. These units, from fault block and basin, have been juxtaposed by the backthrust that carried the Vercors system eastwards onto the Belledonne (Fig. 6). The thermal structure must largely have been established before this Alpine deformation. Note also that the peak temperatures experienced by Jurassic strata in both the hanging wall and footwall to the Meije Thrust are indistinguishable (both are 328°C; Fig. 6). This pattern is consistent with peak temperatures for Jurassic strata that achieved similar burial depths before significant displacement on the thrust.

Bellanger et al.'s (2015) data do however show that the thermal history of the Dauphinois Jurassic strata is more complex than being simply inherited from Mesozoic basin subsidence. Indeed the absolute values would imply burial depths of around 8km, assuming a geothermal gradient of 40 °C /km. Such stratal thicknesses are evident in the Vocontian basin, to the south of the Ecrins (Fig. 2; e.g., de Graciansky et al., 2011), although they are generally regarded as having been greater than those achieved by the Dauphinois successions considered here. Simple uniform stretching models can relate the thicknesses of crust and basin fill (e.g. McKenzie, 1978). The crustal restoration (Fig. 7) implies a stretching factor of 1.34 for the Dauphinois crust, for which a sediment thickness of around 5 km could be accommodated. This however can be increased by inversion and thickening of the basin sediments. 25% shortening, as estimated by Boutoux et al. (2014), increases sediment thicknesses to 6.25 km. For the more eastern sites, further burial may have been achieved by thrust repetition of Jurassic strata. However to achieve temperatures of 330°C a geothermal gradient of around 50°C/km is required during inversion, together with no erosion of the overburden. So, even using the strain values of Boutoux et al. (2014), the choice of appropriate geothermal gradient and the original (pre-inversion) thickness of Mesozoic strata across the Dauphinois basins remain unknown and thus further quantitative consideration of thermal evolution is premature. There are however, other aspects that demand attention.

Strikingly, the Eo-Oligocene units that lie directly upon the Jurassic strata to the east of the study area (Fig. 6) chart maximum temperatures of 298±4 °C,

immediately adjacent to Jurassic strata that record peak temperatures some 40 °C higher. This suggests that the Dauphinois Jurassic strata have experienced two distinct heating episodes. The first of these pre-dates not only the deposition of the Eo-Oligocene strata but also the period of erosion that is represented by its underlying unconformity. The second heating episode was presumably accompanied by tectonic burial by the over-riding thrust sheets derived from the internal Alps and was experienced by the Jurassic and Eo-Oligocene strata together. It is not clear how much of the Dauphinois area experienced this second episode: The full extent of the internal Alpine thrust sheets is not preserved nor are there further Eo-Oligocene deposits preserved across the western Dauphinois area.

The two-phase thermal evolution might be expected to have been recorded by geochronological data. Various radiometric techniques have been applied to establish the timing of Alpine deformation in the Ecrins massif, as recently reviewed by Bellanger et al. (2015). These authors complement existing data with their own substantial data set of Ar-Ar mica ages from selected shear zones within the Ecrins (Fig. 8). The compilation shows significant spread, with a tail of old ages that presumably reflects both the incorporation of old radiogenic Ar from the basement and the incomplete recrystallization of relict mica. However, their study shows a strong cluster of Ar-Ar ages between 20 Ma and 40Ma. Bellanger et al. (2014) suggest that the main deformation phase was at 30-36 Ma. These data do not identify polyphase deformation – an issue to which we shall return after consideration of stratigraphic relationships from the southern Ecrins.

INTEGRATING STRATIGRAPHIC RELATIONSHIPS

The geochronological data pose significant problems for interpreting the deformation history of the Ecrins, when considered alongside stratigraphic relationships. The peak deformation age (30-35 Ma) straddles the late Eocene-early Oligocene (Gradstein et al., 2012). This was the time during which the Nummulitic strata accumulated in the Dauphinois realm. The key location for

493 understanding the relationship between deformation and deposition of these
494 strata lies on the southern flank of the Ecrins, in the Champsaur district (Fig. 9).
495 A regional unconformity at the base of the Nummulitic strata has long
496 been described from the Champsaur district. The unconformity oversteps
497 synclines that hold Jurassic and Triassic strata (e.g. Ford, 1999; Fig. 10a). The
498 Nummulitic strata are folded and overthrust by far-travelled thrust sheets (so-
499 called Embrunais-Ubaye nappes). These relationships are generally interpreted
500 to imply two distinct phases of Alpine tectonics – one "pre-Nummulitic" and
501 another "post-Nummulitic" (e.g. Dumont et al., 2008, 2011). Furthermore, some
502 interpretations infer that the Ecrins massif was continuously high-standing
503 during Alpine deformation, so that it acted not only as a generally rigid
504 obstruction to thrust sheets emplaced from more internal parts of the Alpine
505 chain, but also a barrier to the northward passage of turbidity currents in the
506 ancestral foredeep basin (e.g. Ford and Lickorish, 2004). Consideration of the
507 depositional architecture of the turbidite sandstones of the Champsaur area
508 suggest a different interpretation.
509 The Champsaur district contains two, broadly coeval turbidite sequences
510 contained within two distinct basin areas separated by an Alpine thrust zone
511 (the Selle fault, e.g., Ford, 1999; Fig. 9). The Eastern Champsaur Basin represents
512 a northern continuation of the main Annot sand fairway (Vinnels et al., 2010).
513 Sand compositions are chiefly quartz-rich, consistent with the Annot correlation
514 and are presumed to be similarly sourced from the same Corsican landmass. The
515 island archipelago of Corsica and Sardinia lay immediately south of the modern
516 southern French coast during late Eocene-early Oligocene times (e.g. Joseph and
517 Lomas, 2004). In contrast the Western Champsaur basin has a distinctive
518 volcanic sand component (e.g. Lami et al., 1987; Brunt et al., 2009, and
519 references therein). The structural-stratigraphic relationships of these basins are
520 considered in turn.
521 The Eastern Champsaur basin lies directly beneath thrust sheets derived
522 from the internal Alps and is deformed into a series of WSW-facing folds (e.g.
523 Bürgisser and Ford, 1998). These folds deform the turbiditic component of the
524 Nummulitic succession, detaching along the Blues Marls. The underlying
525 Nummulitic limestone rests unconformably on basement rocks, seen in the

windows of the Fournel and Dourmillouse valleys (Fig. 9a). Local accumulations of continental deposits lie within incised portions of this unconformity, beneath the limestone. Notwithstanding the deformation, regional onlap of the turbidites onto the Blue Marls is evident, so that they are discordant to the underlying Nummulitic limestone. This indicates that the substrate to the Eastern Champsaur Basin was deforming during deposition.

Vinnels et al. (2010) document onlap of the turbidite sandstones and provide paleoflow data collected from their sole structures (Fig. 9). These broadly confirm that the turbidites of the Eastern Champsaur are the northern continuation of the Annot sand fairway (e,g, Sissingh, 2001). The quartz-rich composition of the Champsaur turbidite sandstones is also consistent with this provenance. Paleocurrents indicate that the turbidity currents that supplied the Eastern Champsaur basin were repeatedly deflected by minor intrabasin bathymetry but that overall these flows were not impeded by a basin margin to the north. This means that, during turbidite deposition, the Ecrins massif was not high-standing. Indeed it must have been lower-lying than the Annot basin systems further south in the Alps. But the deflection of individual flows by transient basin-floor bathymetry is consistent with the large-scale stratigraphic motif – that the underlying Ecrins basement was deforming during deposition. This bathymetry could not have been inherited from the Mesozoic for example, as the turbidites of the eastern Champsaur basin are underlain by shallow-water Nummulitic limestone. Furthermore, the onlap angles described by Vinnels et al. (2010) – with 400m of strata pinching out over 4 km – are too high to be explained by regional foredeep flexure alone, especially when decompacted.

The Western Champsaur basin is distinct from the eastern basin because its constituent sandstones are volcaniclastic. Although early stratigraphic syntheses (e.g. Sinclair 1997) assumed these sediments were derived from a now-eroded arc volcanic source in the Alps, paleocurrent and stratigraphic studies indicate a SW provenance, most probably from Oligocene volcanic terrains on Sardinia. Lami et al. (1987) describe the onlap of the sandstones of the western basin onto the Blue Marls together with slumps inferred to have been derived from paleoslopes adjacent to the Ecrins. As with the eastern basin, the onlap angles for the Western Champsaur are too high to be the product of

559 regional flexure alone – and are strongly oblique to the regional foredeep (e.g.
560 Joseph and Lomas; 2003). These stratal relationships (Fig. 10b), together with
561 the systematic decrease in bedding inclination up section, are strong indicators
562 that the southern flank of the Ecrins was deforming during deposition. While this
563 provided a local confining slope to turbidite deposition, the flows continued to
564 pass to the NE, as indicated by paleoflow data (Fig. 9a) together with the
565 geometry of incisional canyons within the system (e.g. Brunt et al., 2007). Thus,
566 as with the Eastern Champsaur Basin, its western counterpart indicates that the
567 adjacent Ecrins massif offered no significant barrier for the passage of turbidity
568 currents in the ancestral foredeep basin and that it continued to deform during
569 their passage.
570 All three lithostratigraphic components of the Nummulitic system are
571 found on the northern side of the Ecrins – with the turbities here known as the
572 Aiguilles d'Arves sandstone (Fig. 3). These units are very poorly described in the
573 literature and have seen no published modern sedimentological studies.
574 Reconnaissance work by the author has discovered a very similar bed-set motif
575 to the turbidites of the Eastern Champsaur Basin. Coarse to medium-grained
576 sandstones are quartz rich. Sole marks imply paleoflow from the south and SE.
577 These observations are consistent with the Aiguilles d'Arves sandstone being
578 further down the same sand fairway as the Eastern Champsaur and Annot
579 systems. It is likely then that, during the deposition of the Aiguilles d'Arves and
580 Eastern Champsaur sandstones, the Ecrins basement did not impede their co-
581 genetic turbidity currents. The down-system continuation of the volcaniclastic
582 turbidites of the Western Champsaur Basin has yet to be identified, although
583 similar rocks are found in the northern Subalps (the Taveyanne Sandstone,
584 reviewed by de Graciansky et al., 2013).
585 The turbidites of both the Eastern and Western Champsaur basins,
586 despite showing distinctly different provenances, both chart deformation of the
587 underlying basement during their deposition. However, both basins also chart
588 deformation that preceded the Nummulitic. Not only has the Mesozoic cover
589 been largely removed by erosion, both basins contain minor amounts of
590 continental deposits directly beneath the Nummulitic limestone that chart
591 subaerial exposure and denudation (e.g. Gupta and Allen, 2000). In the Cedera

592 area the Nummulitic succession of the Western Champsaur basin oversteps folds
593 cored by Triassic and Jurassic strata (e.g. Ford, 1999; Fig. 10a).
594 Field relationships in Champsaur are classically interpreted as the result
595 of two distinct phases of Alpine deformation, separated by a significant period of
596 time represented by the sub-Nummulitic unconformity (e.g. Dumont et al.,
597 2008). The recognition of active basement deformation during turbidite
598 deposition and the long-recognised onlap of tubidites, not onto basement but
599 onto the Blue Marls (Lami et al., 1987), indicates that deformation continued
600 during the Nummulitic. Perhaps the geological history is better explained by
601 continuous rather than episodic deformation.
602
603 **A CONTINUUM MODEL FOR ALPINE DEFORMATION IN THE ECRINS**
604
605 The field relationships in the Champsaur district inspire a model for the
606 tectono-stratigraphic relationships across the Ecrins that may in turn inform
607 discussion of the thermal history (Fig. 11). The section is based on a single
608 hypothetical inverting half graben. This geometry has been proposed for the
609 tract of Jurassic sediments that lie between Combeynot and La Meije basement
610 blocks in the NE of the Ecrins area (e.g. Coward et al., 1991). In this case the
611 hanging wall to the normal fault becomes the Combeynot block. The Mesozoic
612 cover to Combeynot is only found along its western and northern margins. On its
613 eastern side Nummulitic strata lie unconformably on basement. In the model
614 presented here, contractional deformation of the basin began in the mid-to-late
615 Eocene without significant denudation, allowing the Jurassic strata to thicken,
616 burying their deeper portions. It is at this stage that the Jurassic strata achieved
617 their peak temperatures (Fig. 11b). These early parts of the compression are
618 presumably marked either with contractional uplift being outpaced by regional
619 subsidence (e.g. because of flexural loading of the foreland lithosphere) or
620 because there was significant bathymetry across the Mesozoic strata. As
621 deformation continued the evolving, contractional structure was denuded, so
622 that uplift presumably outpaced any regional subsidence (Fig. 11c). Eventually
623 little of the Mesozoic cover was preserved. This stage is marked by the subaerial
624 unconformity at the base of the Nummultitic sequence, during Priabonian (Late

625 Eocene) times. The transgression of this sequence and its progressive foundering
626 charts a period in the continuing deformation where uplift due to contraction
627 was outpaced by regional subsidence – most probably due to flexural loading of
628 the foreland lithosphere (e.g. Ford and Lickorish, 2004). Contractional
629 deformation continued through the accumulation of turbidites across the area
630 (early Oligocene). The deposition terminated with the emplacement of thrust
631 sheets from the internal zones of the Alps. Up until then all the deformation had
632 been emergent. Further deformation of the basin (not illustrated in Fig. 11) will
633 have continued beneath this tectonic cover of thrust sheets but, being buried, is
634 not explicitly recorded by stratigraphic relationships at this location.
635 The kinematic model can be tied to the thermal evolution of the basin. A
636 key result of the analysis of Bellanger et al. (2015; Fig. 6) is that, despite their
637 close proximity, the Nummulitic turbidites north of the Combeynot massif show
638 maximum paleotemperatures c 40 °C lower than their immediately underlying
639 Jurassic substrate. The simplest explanation of these results is that the two units
640 reached their thermal maximum at different times. A qualitative thermal model
641 is presented alongside the kinematic representation (Fig. 11) to illustrate how
642 this might have been achieved.
643 Deformation with different levels of denudation and burial through time
644 is likely to lead to a complex thermal history in the uppermost crust. A more
645 rigorous treatment is currently unwarranted in the absence of heat flow and heat
646 production data for the Ecrins. However, the region probably has values for
647 these parameters that are high relative to most continental crust. The Ecrins
648 basement contains significant volumes of granite and micaceous schists. These
649 units contribute to elevated heat production in analogous basement elsewhere in
650 the Alpine chain (Corsica and Maures-Esterel; e.g., Lucazeau and Vasseur, 1989).
651 Deville and Sassi (2006) use the relatively high heat flow estimate of 80mW per
652 square metre for their models for hydrocarbon maturation in the Vercors. High
653 heat production in basement and high heat flow into the overlying cover units is
654 likely to lead to elevated near surface temperatures during periods of
655 denudation (Fig. 11c) and, for subsequent burial under thrust sheets (Fig. 11e),
656 rapid re-heating of the Jurassic strata. That these strata did not achieve their
657 thermal maximum during this subsequent burial suggests that the overlying

thrust sheet was substantially denuded relatively soon after its emplacement, as deformation continued into the Miocene.

THE ALPINE SUBDUCTION CHANNEL AND CONTINUOUS FORELAND DEFORMATION

The pattern of long-lived continuous deformation and tectonic inversion within the external basement massifs can now be placed in a broader Alpine context (Fig. 12). Although this deformation straddled the Eocene-Oligocene boundary (c. 34 Ma, Gradstein et al., 2012), it is unclear how much earlier it started. Elsewhere in the Annot system deformation appears to have begun only after the Nummulitic transgression (e.g. Salles et al., 2014) – suggesting an onset only within the Priabonian (i.e., after 38 Ma, Gradstein et al., 2012). Thus most plausibly deformation in the Ecrins began in the Priabonian (around 37±1 Ma). Likewise the termination of significant deformation within the Dauphinois basins is difficult to establish, although consideration of the Ar-Ar data (Fig. 8) indicate it had ended by 20 Ma. Bellanger et al. (2015) suggest that deformation was concentrated in the period of c 36-30 Ma during the Oligocene. After this time, it is likely that deformation had localised onto the Basal Belledonne Thrust (Fig. 7) and that this simply elevated the Ecrins massif, as charted by its late-stage denudation history (van der Beek et al., 2010). Therefore deformation of the Ecrins basement was probably protracted over a period of 6-10 Myr during which time around 35 km of crustal shortening was accommodated. The shortening rate was therefore around 0.35 - 0.5 cm/yr.

While the Nummulitic succession was being accumulated across the inverting Dauphinois basins, the more distal parts of the former rifted continental margin of Europe were being taken into the subduction channel of the Alps. Peak burial to 3.5-4.4 GPa of the Dora Maira massif, equating to depths of c 120 km, is dated at 34-35 Ma (reviewed by McClelland and Lappin, 2013). Exhumation to c. 1.5 GPa (c 45 km depth) occurred within the following 2-3 Myr, at rates of 2-3 cm/yr. Thus both the original subduction of continental crust and a significant part of its exhumation within the subduction channel was coeval with crustal shortening in the Ecrins (Fig. 12). However, only a small part of the

691 exhumation of the Dora Maira massif could have been accompanied by thrusting
692 in the external basement massifs. Significantly more displacement may have
693 been partitioned onto the Frontal Pennine Thrust and yet more within the
694 internal Alps. Establishing these displacements is a task for future investigations.
695
696 **DISCUSSION**
697
698 The study presented here confirms and develops the general notion that
699 the former rifted margin structure of Europe influenced the tectonic evolution of
700 the western Alps (Gillcrist et al., 1987; Butler et al., 2006; Bellahsen et al., 2014).
701 For the former Dauphinois basins, contractional deformation was broadly
702 distributed within the upper crust and unlike some other basin settings, did not
703 localise exclusively onto the pre-existing extensional fault systems (Coward et
704 al., 1991; Butler et al., 2006). Area balancing the crust beneath the external
705 Western Alps, with the assumptions of whole crustal deformation and plane
706 strain, gives a prediction of the pre-orogenic crustal thickness and therefore an
707 estimate of stretching factors during the earlier development of the rifted
708 margin. These restorations are broadly consistent with illustrations of crustal
709 thickness on qualitative representations of this part of the former rifted
710 continental margin of Europe (e.g. Lemoine et al., 1986; Mohn et al., 2010).
711 The key conclusion here is that inversion of the Dauphinois basins was
712 protracted, continuing for c. 6-10 Myr. Much of this deformation was distributed
713 with no discernable “sequence”. There is no evidence for simple forelandward
714 migration of inversion. Rather deformation appears to have been continuous,
715 only localising onto a few structures (the Combeynot, La Meije and Basal
716 Belledonne thrusts). This deformation occurred in tandem with subduction and
717 exhumation of originally more distal (oceanward) parts of the former
718 continental margin of Europe. This synchronicity of deformation within the
719 former continental margin is consistent with previously hypothetical predictions
720 of how the inherited heterogeneous structure can influence deformation styles
721 and timing (Butler, 2013; Fig. 1).
722 Descriptions of deformation within mountain belts have generally
723 inferred a simple forelandward migration (e.g. Ford and Lickorish, 2004).

724 However, in regions where deformation can be dated directly by stratigraphic
725 relationships in syn-kinematic deposits (e.g. Butler and Lickorish, 1997 and
726 references therein), simple thrust sequences are not evident. Rather deformation
727 can be shown to have occurred synchronously across an array of folds.
728 Furthermore, distributions of earthquakes and geodetic measurements reveal
729 that, in the modern world, active contraction does not simply occur on a single
730 structure. These data too show broadly synchronous activity across an array of
731 faults (e.g. Ansari and Zamani, 2014). The deductions for structural evolution in
732 the Ecrins presented here are consistent with these studies.
733 Classical stratigraphic approaches of deducing the timing of tectonics rely
734 on unconformities (e.g. Stille, 1924), a focus that has fostered consideration of
735 orogenic evolution as a progression of distinct events. This is misleading as
736 unconformities in progressive deformation simply chart the interplay between
737 erosion and this deformation. The recognition of growth strata is critical – but
738 complex - as different styles of deposition, both in terms of distribution and rate,
739 create different growth stratal patterns (e.g. Butler and Lickorish, 1997), which
740 necessitate protracted stratigraphic studies. These may be difficult where the
741 key strata subsequently become incorporated into the developing orogen. Within
742 the Alpine system, the syn-kinematic status of various successions is becoming
743 recognised (e.g. Salles et al., 2014). But in many settings these succession have
744 been eroded during subsequent periods of deformation.
745 A complementary approach to using stratigraphy to chart deformation
746 histories is to integrate geochronology, such as the study of Bellanger et al.
747 (2015) used here. The limitation, however, is that a few spot-dates may be
748 insufficient for tracking the deformation activity and its migration across an
749 array of structures. This is equivalent to obtaining a few biostratigraphic ages for
750 a sedimentary succession. Without establishing the stratal geometries, the
751 necessary deduction of syn-kinematic successions is highly ambiguous. The
752 challenge for evaluating the timescales for continuous deformations is to develop
753 better investigative strategies that incorporate substantially larger and more
754 diverse datasets.
755
756 **ACKNOWLEDGEMENTS**

The account presented here is based on many years of Alpine research by the author and numerous discussions with individuals on Alpine and other tectonics. I especially thank Bill McCaffrey and others within the Leeds Turbidites Research Group for initiating me in the ways of deep marine clastic sedimentology. Mark Cooper and Steve Matthews are thanked for their acute comments on an earlier draft of this manuscript. I also thank editor Rick Law for his patience with this manuscript.

REFERENCES CITED

Ansari, S., and Zamani, A., 2014, Short-term seismic crustal deformation of Iran: Annales of Geophysics, v. 57, doi:10.4401/ag-6413.

Barféty, J.C., Gidon, M., Lemoine, M., and Mouterde, R., 1979, Tectonique synsédimentaire liasique dans les massifs cristallins de la zone externe des Alpes occidentales francaises: la faille du col d'Ornon: Comptes rendus de l'académie des sciences, Paris, v. 289, p. 1207-1210.

Bayer, R., Cazea, M., Dal Piaz, G.V., Damotte, B., Elter, G., Gosso, G., Alfred, H., Lanza, R., Lombardo, B., Mugnier, J-L., Nicolas, A., Nicolich, R., Polino, R., Roure, F., Sacchi, R., Scarascia, S., Tobacco, I., Tapponnier, P., Tardy, M., Taylor, M., Thouvenot, F., Toreilles, G., and Villien, A., 1987, Premiers résultats de la traversée des Alpes occidentales par sismique reflexion vertical (Programme ECORS-CROP): Comptes rendus de l'académie des sciences, Paris, v. 305, p. 1461-1470.

Beach, A., 1981, Thrust structures in the eastern Dauphinois Zone (French Alps), north of the Pelvoux Massif: Journal of Structural Geology, v. 3, p. 299-308.

van der Beek, P.A., Valla, P.G., Herman, F., Braun, J., Persano, C., Dobson, K.J., and Labrin, E. 2010, Inversion of thermochronological age-elevation profiles to extract independent estimates of denudation and relief history – II: Application to the French Western Alps: Earth and Planetary Science Letters, v. 296, p. 9-22.

Bellahsen, N., Jolivet, L., Lacombe, O., Bellanger, M., Boutoux, A., Garcia, S., Mouthereau, F., Le Pourhiet, L., and Gumaix, C., 2012, Mechanisms of

margin inversion in the external Western Alps: Implications for crustal rheology: Tectonophysics, v. 560-561, p. 62-83.

Bellahsen, N., Mouthereau, F., Boutoux, A., Bellanger, M., Lacombe, O., Jolivet, L., and Rolland, Y., 2014, Collision kinematics in the western Alps: Tectonics, v. 33, p. 1055-1088.

Bellanger, M., Augier, R., Bellahsen, N., Jolivet, L., Monié, P., Baudin, T., and Beyssax, O., 2015, Shortening of the European Dauphinois margin (Oisans Massif, Western Alps): New insights from RSCM maximum temperature estimates and $^{40}Ar/^{39}Ar$ in situ dating: Journal of Geodynamics, v. 83, p. 37-64.

Boutoux, A., Bellahsen, N., Lacombe, O., Verlaguet, A., and Mouthereau, F, 2014, Inversion of pre-orogenic extensional basins in the external Western Alps: Structure, microstructures and restoration: Journal of Structural Geology, v. 60, p. 13-29.

Brunt, R.L., McCaffrey, W.D., and Butler, R.W.H., 2007, Setting and architectural elements of the Champsaur Sandstones, France, *in* Nilsen, T.H., Shew, R.D., Steffens, G.S., and Studlick, J.R.J., eds., Atlas of deep-water outcrops: American Association of Petroleum Geologists Studies in Geology, v. 56, p. 188-191.

Bürgisser, J., and Ford, M., 1998, Overthrust shear deformation of a foreland basin; structural studies south-east of the Pelvoux massif, SE France: Journal of Structural Geology, v. 20, p. 1455–1475.

Butler, J.P., Beaumont, C., and Jamieson, R.A., 2013, The Alps 2: Controls on crustal subduction and (ultra) high-pressure rock exhumation in Alpine-type orogens: Journal of Geophysical Research: Solid Earth, doi:10.1016/j.epsl.2013.06.039.

Butler, R.W.H., 1986, Thrust tectonics, deep structure and crustal subduction in the Alps and Himalayas: Journal of the Geological Society, London, v. 143, p. 857-873.

Butler, R.W.H., 1987, Thrust system evolution within previously rifted areas: an example from the Vercors, French subalpine chains: Memorie della Societa Geologica Italiana, v. 38, p. 5-18.

822 Butler, R.W.H., 1989, The influence of pre-existing basin structure on thrust system
823 evolution in the western Alps, *in* Cooper, M.A., and Williams, G.D., eds.,
824 Inversion Tectonics: Special publications of the Geological Society, London, v
825 44, p.105-122.
826 Butler, R.W.H., 1992, Thrusting patterns in the NW French Subalpine chains:
827 Annales. Tectonicae, v. 6, p. 150-172.
828 Butler, R.W.H., 2013, Area balancing as a test of models for the deep structure of
829 mountain belts, with specific reference to the Alps: Journal of Structural
830 Geology, v. 52, p. 2-16.
831 Butler, R.W.H., and Lickorish, W.H., 1997, Using high resolution stratigraphy to date
832 fold and thrust activity: examples from the Neogene of South-central Sicily
833 Journal of the Geological Society, London, v. 154, p. 633-643.
834 Butler, R.W.H., Matthews, S.J., and Parish, M., 1986, The NW external Alpine thrust
835 belt and its implications for the geometry of the Western Alpine orogeny, *in*
836 Coward, M.P., and A.C. Ries, A.C., eds., Collision Tectonics: Special publications
837 of the Geological Society, London, v. 19, p. 245-263.
838 Butler, R.W.H., Tavarnelli, E., and Grasso, M., 2006, Structural inheritance in
839 mountain belts: an Alpine-Apennine perspective: Journal of Structural Geology,
840 v. 28, p. 1893-1908.
841 Cavazza, W., Roure, F., and Ziegler, P.A., 2004, The Mediterranean area and
842 sutrounding regions: active processes, remnants of former Tethyan oceans and
843 related thrust belts, *in* W. Cavazza, Roure, F.M., Spakman, W., Stampfli, G.M., and
844 Ziegler, P.A., eds., The Transmed Atlas: the Mediterranean region from crust to
845 mantle: Springer, p. 1-18.
846 Clavel, B., Conrad, M.A., Busnardo, R., Charollais, J. and Granier, B., 2013, Mapping
847 the rise and demise of Urgonian platforms (Late Hauterivian – Early Aptian) in
848 southeastern France and the Swiss Jura: Cretaceous research, v. 39, p. 29-46.
849 Coward, M.P., Gillcrist, R., and Trudgill, B., 1991, Extensional structures and their
850 tectonic inversion in the Western Alps, in Roberts, A.M., Yielding, G., and
851 freeman, B., eds., The Geometry of Normal Faults: Special publications of the
852 Geological Society, London, v. 56, p. 93-112.

853 Deville, E., and Sassi, W., 2006. Contrasting thermal evolution of thrust systems: An
854 analytical and modelling approach in the front of the western Alps: Bulletin of
855 the American Association of Petroleum Geologists, v. 90, p. 889-907.
856 Dumont, T., Champagnac, J-D., Crouzet, C., and Rochat, P., 2008. Multistage
857 shortening in the Dauphiné zone (French Alps): the record of Alpine collision
858 and implications for pre-Alpine restoration: Swiss Journal of Geosciences, v.
859 101, p. S89-S110.
860 Dumont, T., Simon-Labric, T., Authemayou, C., and Heymes, T., 2011. Lateral
861 termination of the north-directed Alpine orogeny and onset of westward
862 escape in the western Alpine arc: Structural and sedimentary evidence from the
863 external zone: Tectonics, v. 30, TC5006.
864 Ford, M., 1999, Kinematics and geometry of early Alpine, basement-involved folds,
865 SW Pelvoux Massif, SE France: Ecologae Geologicae Helvetiae (Swiss Journal of
866 Geosciences), v. 89, p. 269-295.
867 Ford, M., and Lickorish, H., 2004, Foreland basin evolution around the western
868 Alpine arc, *in* Joseph, P., and Lomas, S.A., eds., Deep-water sedimentation in the
869 Alpine Foreland Basin of SE France: New perspectives on the Grès d'Annot and
870 related systems: Special publications of the Geological Society, London, v. 221,
871 p. 39-63.
872 François, D., and Lemmet, M., 1999, Evolution of Mg/Fe ratios in late Variscan
873 plutonic rocks from the external crystalline massifs of the Alps (France, Italy,
874 Switzerland): Journal of Petrology, v. 40, p. 1151-1185.
875 Gidon, M., 1977, Carte géologique simplifiée des Alpes occidentales, du Léman à
876 Digne, au 1/250.000°: éditions Didier Richard and B.R.G.M., Orleans.
877 Gidon, M., Arnaud, H., Pairis, J-L., Aprahamian, J., and Uselle, J-P., 1970, Les
878 déformations tectoniques superposées du Dévoluy méridonial (Hautes-Alpes):
879 Geologie Alpine, v. 46, p. 87-110.
880 Gillcrist, R., Coward, M.P., and Mugnier, J-L., 1987, Structural inversion: examples
881 from the Alpine foreland and French Alps: Geodinamica Acta, v. 1, p. 5-34.
882 de Graciansky, P-C., Roberts, D.G., and Tricart, P., 2011, The Western Alps, from rift
883 to passive margin to orogenic belt: Developments in Earth Surface Processes, v.
884 14, pp. 1-398.

885 Gradstein, F.M., Ogg, J.G., and Hilgen, F.J., 2012, On the geologic timescale:
886 Newsletters on Stratigraphy, v. 45/2, p. 171-188.
887 Gratier, J-P., Ménard, G., and Arpin, R., 1989, Strain-displacement compatibility and
888 restoration of the Chaînes Subalpines of the western Alps, *in* Coward, M.P.,
889 Dietrich, D., and Park, R.G., eds., Alpine Tectonics: Special publications of the
890 Geological Society, London, v. 45, p. 65-81.
891 Hatcher, R.D., and Hooper, R.J., 1992, Evolution of crystalline thrust sheets in the
892 internal parts of mountain chains, *in* McClay. K.R., ed., Thrust tectonics:
893 Chapman and Hall, London, p. 217-234.
894 Gupta, S., and Allen, P.A., 2000, Implications of foreland paleotopography for
895 stratigraphic development in the Eocene distal Alpine foreland basin:
896 Geological Society of America, Bulletin, v. 112, p. 515–530.
897 Hill, K.C., and Hall, R., 2002, Mesozoic-Cainozoic evolution of Australia's New
898 Guinea margin in a west Pacific context, *in* Hillis, R., and Müller, R.D., eds.,
899 Defining Australia: The Australian Plate: Geological Society of America
900 Special Paper, v. 372, p. 259-283.
901 Joseph, P., and Lomas, S.A., 2004, Deep-water sedimentation in the Alpine Foreland
902 Basin of SE France: New perspectives on the Grès d'Annot and related systems
903 – an introduction, *in* Joseph, P., and Lomas, S.A., eds., Deep-water
904 sedimentation in the Alpine Foreland Basin of SE France: New perspectives on
905 the Grès d'Annot and related systems: Special publications of the Geological
906 Society, London, v. 221, p. 1-16.
907 Lami, A., Fabre, P., Pairis, J-L., and Gidon, M., 1987, Les caractères du détritisme
908 paléogène aux abords du massif du Pelvoux (Alpes externes méridionales):
909 Géologie alpine, v. 13, 319-328.
910 Lemoine, M., Bas, T., Arnaud-Vanneau, A., Arnaud, H., Dumont, T., Gidon,, M.,
911 Bourbon, M., de Graciansky, P.C., Rudkiewicz, J.L., Megard-Galli, J., and
912 Tricart, P., 1986, The continental margin of the Mesozoic Tethys in the
913 Western Alps: Marine and Petroleum Geology, v. 3, p. 179–199.
914 Lucazeau, F., and Vasseur, G., 1989, Heat flow density data from France and
915 surrounding margins: Tectonophysics, v. 164, p. 251 – 258.
916 McBride, J.H., Hatcher, R.D., Stephenson, W.J., and Hooper, R.J., 2005, Integrating
917 seismic reflection and geological data and interpretations across an internal

basement massif: The southern Appalachian Pine Mountain window, USA: Bulletin of the Geological Society of America, v. 117, p. 669-686.

McClelland, W.C., and Lappin, T.J., 2013, Linking time to the pressure-temperature path of Ultrahigh-Pressure rocks: Elements, v. 9, p. 273-279.

McKenzie, D., 1978, Some remarks on the development of sedimentary basins: Earth and Planetary Science Letters, v. 40, p. 25-32.

Mohn, G., Manatschal, G., Muntener, O., Beltrando, M., and Masini, E., 2010, Unravelling the interaction between tectonic and sedimentary processes during lithospheric thinning in the Alpine Tethys margins: International Journal of Earth Science, v. 99, p. S75-S101.

Pashin, J.C., Kopaska-Merkel, D.C., Arnold, A.C. McIntyre, M.R., and Thomas, W.A., 2012, Gigantic, gaseous mushwads in Cambrian shale: Conasauga Formation, southern Appalachians, USA: International Journal of Coal Geology, v. 103, p. 70-91.

Péron-Pinvidic, G., and Manatschal, G., 2010, From microcontinents to extensional allochthons: witness of how continents rift and break apart: Petroleum Geoscience, v. 16, 189-197.

Phillippe, Y., Deville, E., and Mascle, A., 1998. Thin-skinned inversion tectonics at oblique basin margins: example of the western Vercors and Chartreuse Subalpine massifs (SE France), *in* Mascle, A., Puigdefabregas, C., Luterbacher, H.P., and Fernandez, M., eds., Cenozoic Foreland Basins of western Europe: Special publications of the Geological Society, London, v. 134, p. 239-262.

Ramsay, J.G. 1963, Stratigraphy, structure and metamorphism in the Western Alps: Proceedings of the Geologists' Association, v. 74, p. 357-391.

Raumer, J.F. von, Bussy, F., and Stampfli, G.M., 2009, The Variscan evolution in the External massifs of the Alps and place in their Variscan framework: Comptes Rendus Geoscience, v. 341, p. 239-252.

Roure, F., Choukroune, P., Berastegui, X., Munoz, J.A., Villien, A., Matheron, P., Bareyt, M., Seguret, M., Camara, P., and Deramond, J., 1989, ECORS deep seismic data and balanced cross-sections: geometric constraints on the evolution of the Pyrenees: Tectonics, v. 8, p. 41-50.

949 Salles, L., Ford, M., and Joseph, P., 2014. Characteristics of axially-sourced turbidite
950 sedimentation on an active wedge-top basin (Annot Sandstone, SE France):
951 Marine and Petroleum Geology, v. 56, p. 305-323.
952 Schmid, S.M., and Kissling, E., 2000, The arc of the western Alps in the light of
953 geophysical data on deep crustal structure: Tectonics, v. 19, p. 62-85.
954 Schmid, S.M., Fügenschuh, B., Kissling, E., and Schuster, R., 2004, Tectonic map and
955 overall architecture of the Alpine orogeny: Eclogae geologicae Helvetiae, v. 97,
956 p. 93-117.
957 Schulmann, K., Martinez Catalan, J.R. Lardeaux, J.M., Janousek, V., and Oggiano, G.
958 (eds), 2014, The Variscan Orogeny: Extent, timescale and the formation of the
959 European Crust: Special Publications of the Geological Society of London, v.
960 405, pp. 400.
961 Sinclair, H.D., 1997, Tectonostratigraphic model for underfilled peripheral foreland
962 basins: An Alpine perspective: Geological Society of America Bulletin, v. 109, p.
963 324-346.
964 Sissingh, W., 2001, Tectonostratigraphy of the West Alpine foreland: correlation of
965 Tertiary sedimentary sequences, changes in eustatic sea-level and stress
966 regimes: Tectonophysics, v. 333, p. 361-400.
967 Stille, H., 1924, Grundfragen der vergleichenden Tektonik: Borntraeger, Berlin, pp.
968 443.
969 Vinnels, J.S. Butler, R.W.H., McCaffrey, W.D., and Lickorish, W.H., 2010, Sediment
970 distribution and architecture around a bathymetrically complex basin:
971 Eastern Champsaur Basin, SE France: Journal of Sedimentary Research, v.
972 80, p. 216-235.
973 Wibberley, C.A.J., 1997, A mechanical model for the reactivation of
974 compartmental faults in basement thrust sheets, Muzelle region, Western
975 Alps: Journal of the Geological Society, London, v. 154, p. 123-128.
976 Zhao, L., Paul, A., Guillot, S., Solarino, S., Malusà, M.G., Zheng, T., Aubert, C.,
977 Salimbeni, S., Dumont, T., Schwartz, S., Zhu, R., and Wang, Q., 2015, First
978 seismic evidence for continental subduction beneath the Western Alps:
979 Geology, v. 43, p. 815-818.
980
981

Figures

Figure 1. Schematic model for the timing of deformation (a-c in time) in a subduction channel containing segments of an originally rifted continental margin. Modified after Butler (2013). X represents the leading edge of the down-going rifted continental margin (e.g. future Dora Maira massif of Western Alps). Y represents the former oceanward extent of the weakly rifted continental crust (future external basement massifs of the Western Alps). Ellipses qualitatively represent strain states within the crust.

Figure 2. Simplified geo-tectonic map of the western Alps (modified after Schmid et al., 2004), showing locations discussed in the text. DT = Digne Thrust.

Figure 3. Simplified geological map of the external basement massifs centred on the Ecrins (chiefly after Gidon, 1977). See Fig. 2 for location.

Figure 4. Compilation of interpretations of basement-cover relationships in the Ecrins area. a) Ramsay's (1963) concept of "pinched-in synclines"; b) Beach's (1981) thrust model; c) Coward et al.'s (1991) vision of tectonic inversion of Jurassic fault blocks; d) Dumont et al.'s (2008) model of heterogeneous distributed strain; e) Bellahsen et al.'s (2012) model of simple-shear dominant deformation in the basement.

Figure 5. Basement cover relationship in the Ecrins district. a) Classical view looking SE (e.g. Lemoine et al., 1986) of the Ornon fault in its type location (La Chalp village). The fault plane is represented by the main escarpment, with the gentle low ground containing the Jurassic sediments of the Ornon basin. The visible hillside (eastern margin of the Taillefer basement block) is c 1700m high. b) detail of the Ornon fault (boxed area on Fig. 5a) showing the Jurassic fault plane (figures for scale, reverse angle to Fig. 5a). The hanging wall to the fault contains deformed sedimentary breccias of Jurassic age with a pronounced slaty cleavage that is sub-parallel to the

plane of the Ornon Fault. c) Looking east into the upper Romanche valley above the village of La Grave. Most units dip away from the viewer. The foreground contain the Emparis basement block, overlain by its sedimentary cover (chiefly Jurassic shales). These in turn are tectonically overlain by the La Meije basement, carried on the La Meije Thrust (MT). This basement unit is overthrust by the Combeynot Thrust (CT) that carries the Combeynot Bock (CB). Note that the main thrusts climb laterally (northwards) in their hanging walls, from basement out into Jurassic cover rocks.

Figure 6. Simplified regional cross section (located on Fig. 3) showing the chief structural elements in the external western Alps, along a transect from the Vercors to the Frontal Pennine Thrust just east of the Combeynot massif (Fig. 5). The thermal data are after Bellanger et al. (2015) and display peak temperatures recorded in sedimentary rocks.

Figure 7. A simplified balanced and restored cross section for the continental crust along the Ecrins-Vercors transect (Fig. 6). See text for discussion.

Figure 8. Compilation of Ar-Ar age data from the Ecrins and Combeynot areas, after Bellanger et al. (2015).

Figure 9. a) Simplified geological map of the southern Ecrins district showing the two Champsaur turbidite basins. Paleoflow data is after Brunt et al. (2007) and Vinnels et al. (2010). The section (b) is after Gidon (Géol. Alp website).

Figure 10. Relationships between the Nummulitic succession and its substrate in the southern Ecrins. The viewpoints are shown on Fig. 9. a) looking onto the west face of Cedera from the hamlet of Les Fermons (c 1400m). b) looking towards the main tract of the Western Champsaur Basin from Sommet Drouvet (2655m). The lolly-pops denote bedding dip.

Figure 11. Schematic tectono-thermal model for continuous deformation (a-e in time) of the Ecrins domain – based on structural and stratigraphic relationships applied to a single inverting half-graben. J represents Jurassic strata on the thermal model, while e represents the Eo-Oligocene strata. See text for further details.

Figure 12. Placing the Ecrins in a subduction channel context. a) is a schematic illustration of the rifted European continental margin before orogenic contraction (after Butler, 2013). b) schematically illustrates the tectonic situation at c 34 Ma, as Dora Maira achieves its peak burial while deformation progresses with inversion of the former Dauphinois basins, at the mouth of the subduction channel. Subsequent return flow of the Dora Maira crust as a pip within the subduction channel generates significant "late" deformation in units further up (as sketched in Fig. 1c).

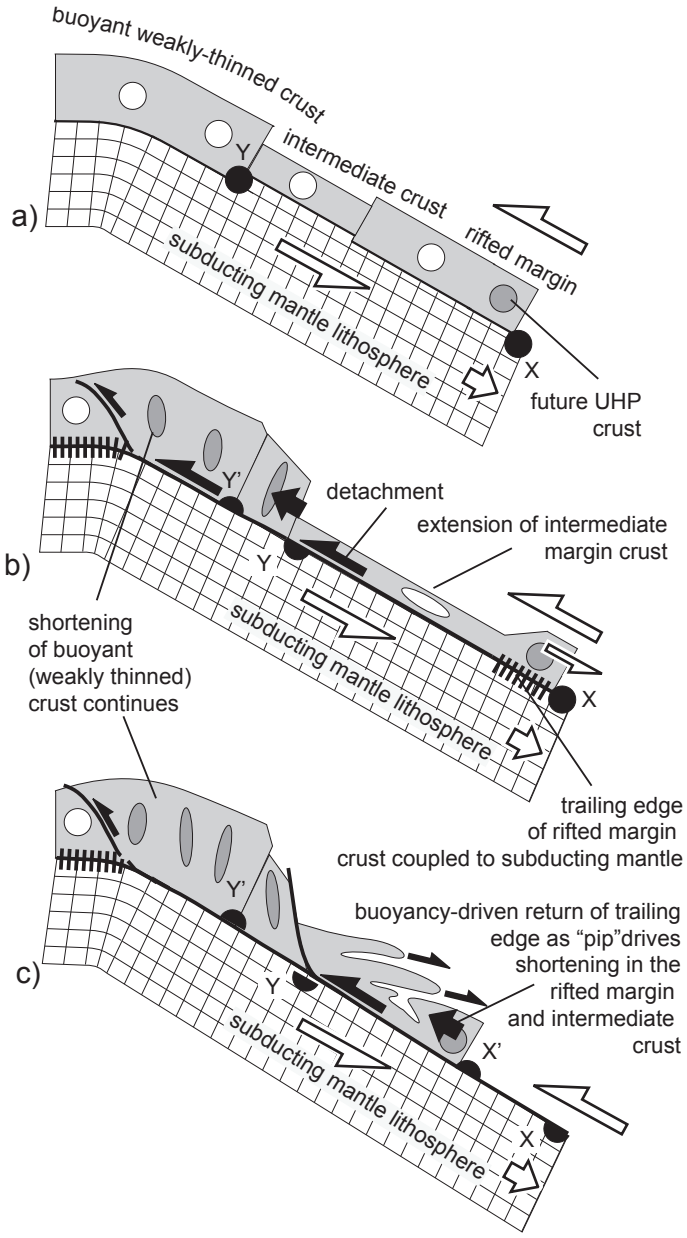
buoyant weakly-thinned crust
intermediate crust
rifted margin
a)
Y
X
subducting mantle lithosphere
future UHP crust
Y'
detachment
extension of intermediate margin crust
b)
Y
X
shortening of buoyant (weakly thinned) crust continues
subducting mantle lithosphere
trailing edge of rifted margin crust coupled to subducting mantle
Y'
buoyancy-driven return of trailing edge as "pip"drives shortening in the rifted margin and intermediate crust
c)
Y
X'
subducting mantle lithosphere
X

Figure 1.

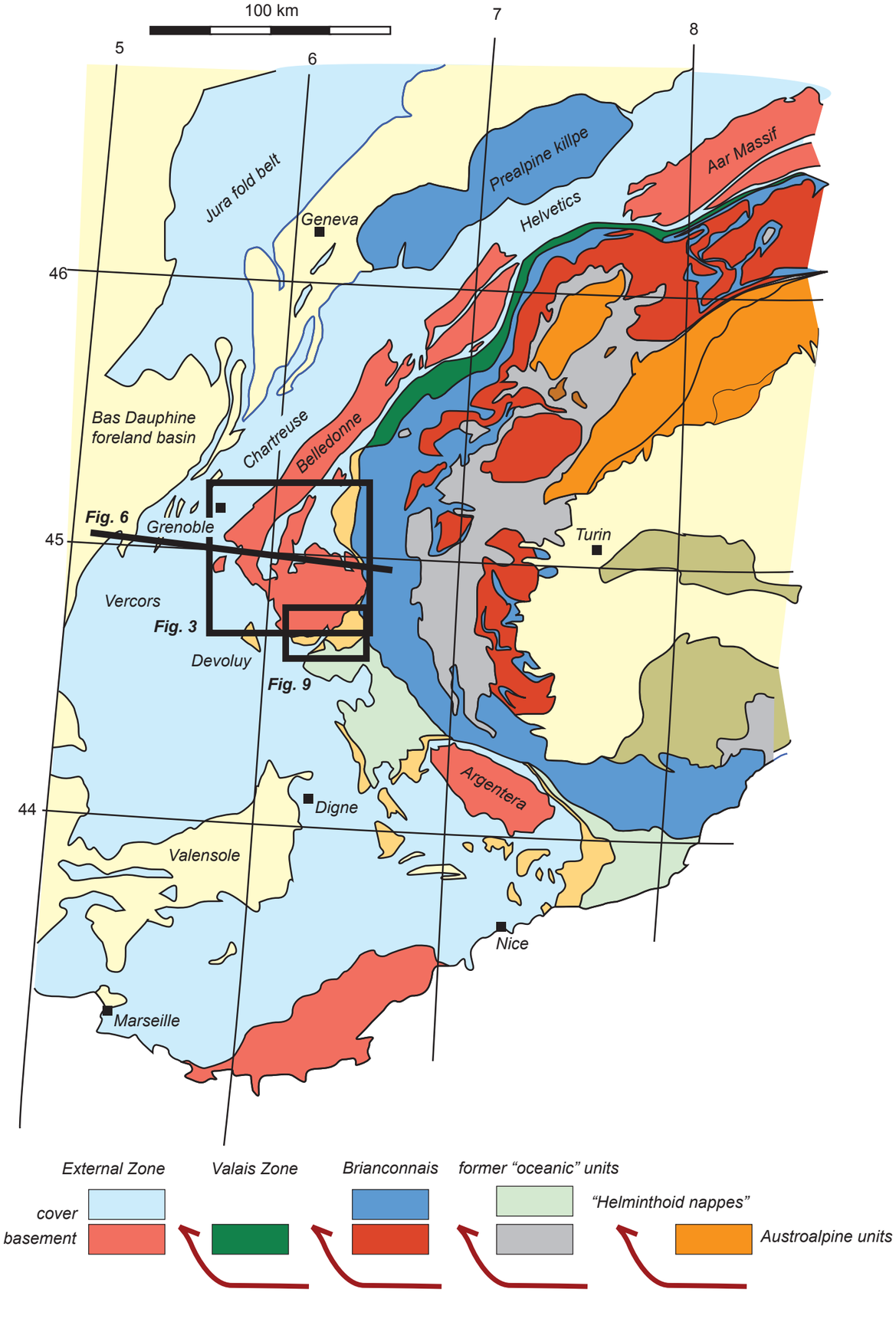
100 km
5
6
7
8
46
45
44
Jura fold belt
Geneva
Prealpine klippe
Helvetics
Aar Massif
Bas Dauphine
foreland basin
Chartreuse
Belledonne
Fig. 6
Grenoble
Turin
Vercors
Fig. 3
Devoluy
Fig. 9
Argentera
Digne
Valensole
Nice
Marseille
External Zone
Valais Zone
Brianconnais
former "oceanic" units
"Helminthoid nappes"
cover
basement
Austroalpine units

Figure 2

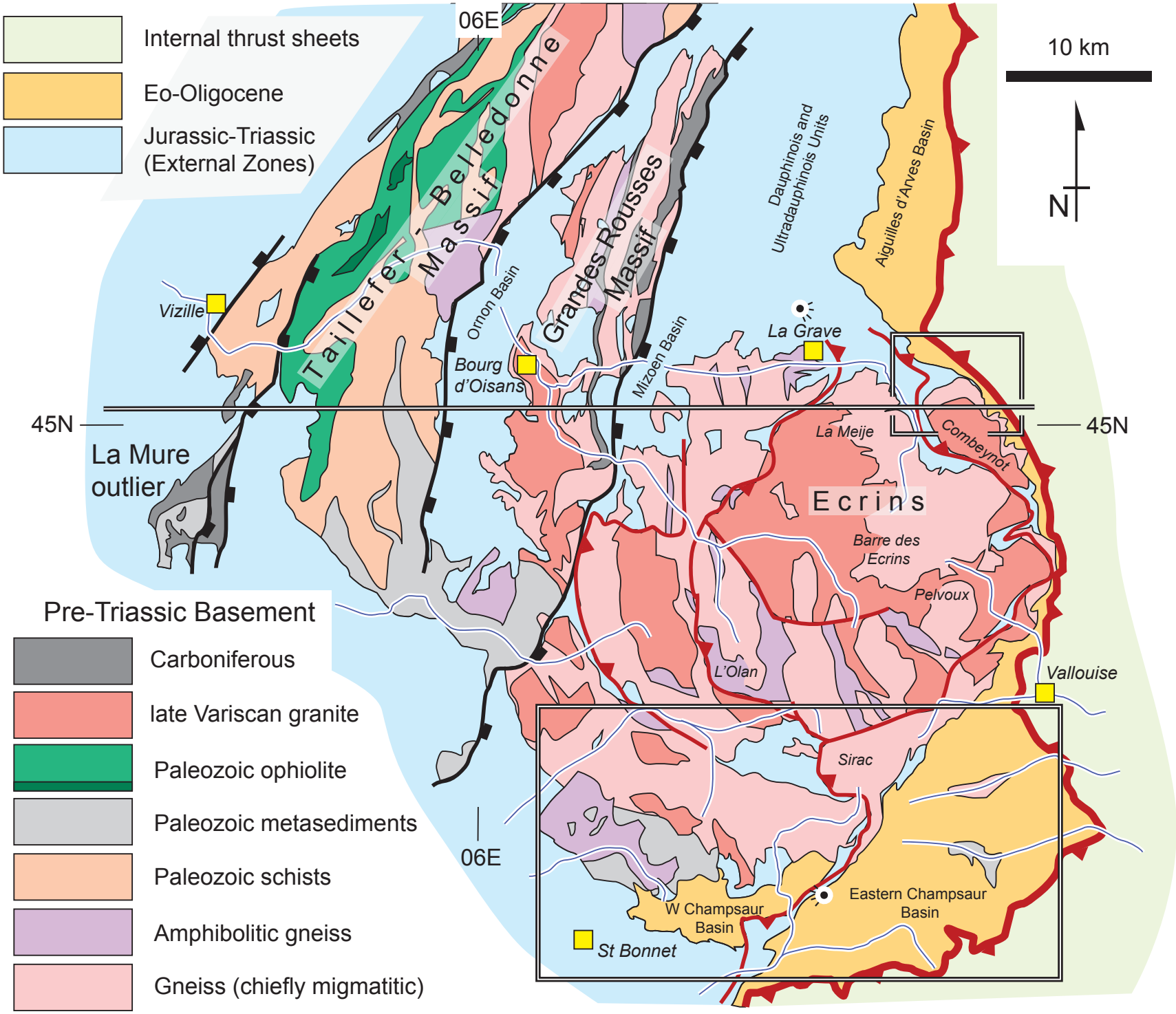
Internal thrust sheets
Eo-Oligocene
Jurassic-Triassic
(External Zones)
Pre-Triassic Basement
Carboniferous
late Variscan granite
Paleozoic ophiolite
Paleozoic metasediments
Paleozoic schists
Amphibolitic gneiss
Gneiss (chiefly migmatitic)
06E
10 km
N
45N
45N
06E
Taillefer - Belledonne Massif
Grandes Rousses Massif
Dauphinois and Ultradauphinois Units
Aiguilles d'Arves Basin
Ornon Basin
Mizoen Basin
Vizille
Bourg d'Oisans
La Grave
La Mure outlier
La Meije
Combeynot
Ecrins
Barre des Ecrins
Pelvoux
L'Olan
Vallouise
Sirac
W Champsaur Basin
Eastern Champsaur Basin
St Bonnet

Figure 3

Figure 4

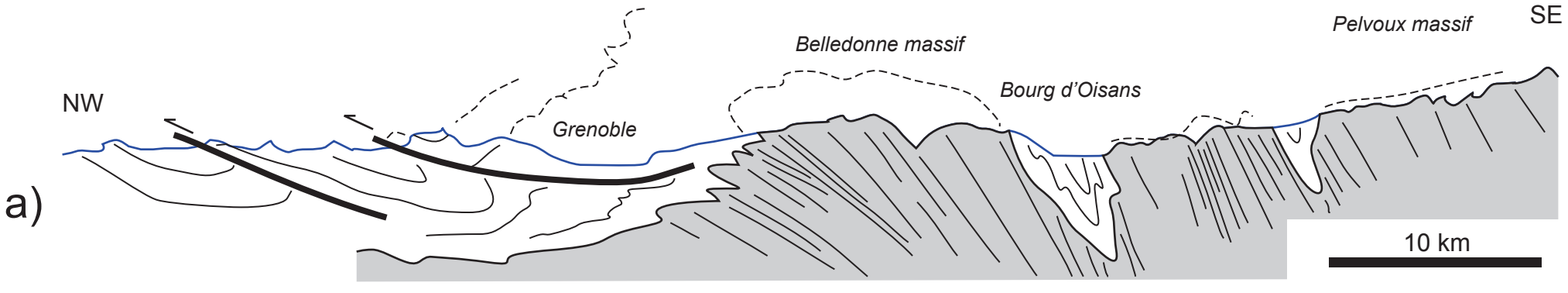

a)

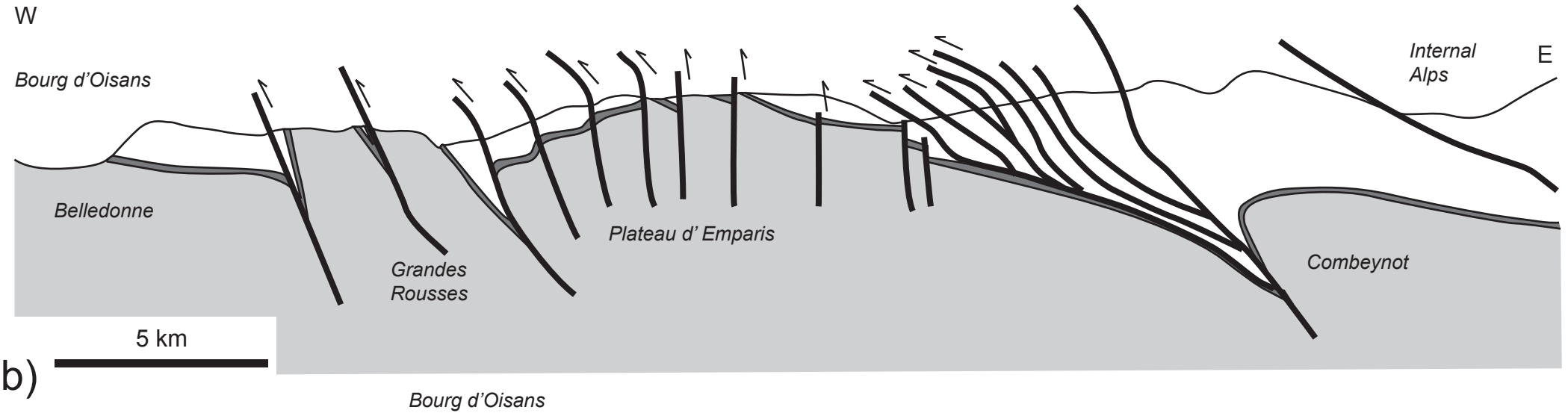

b)

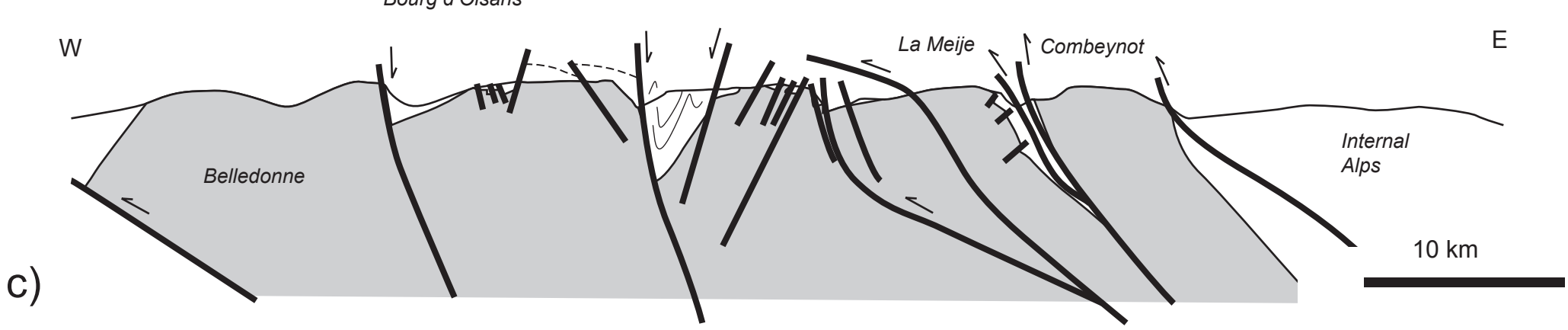

c)

E

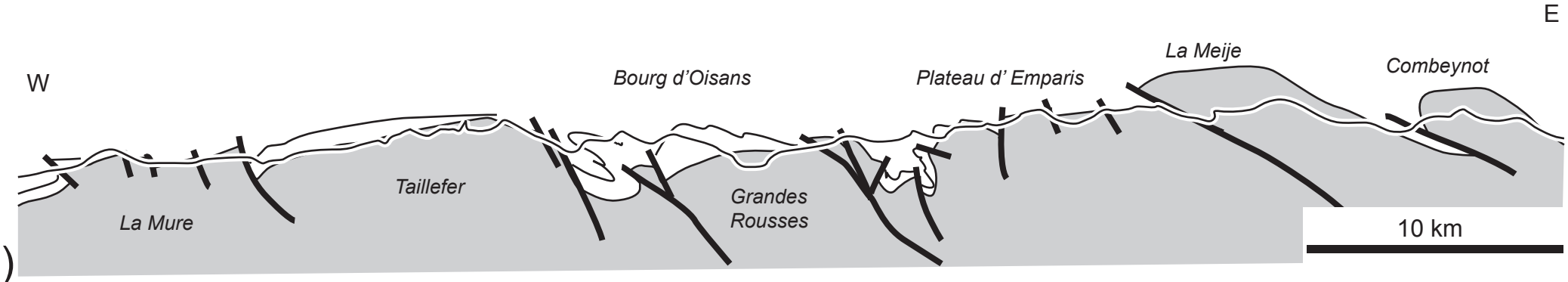

d)

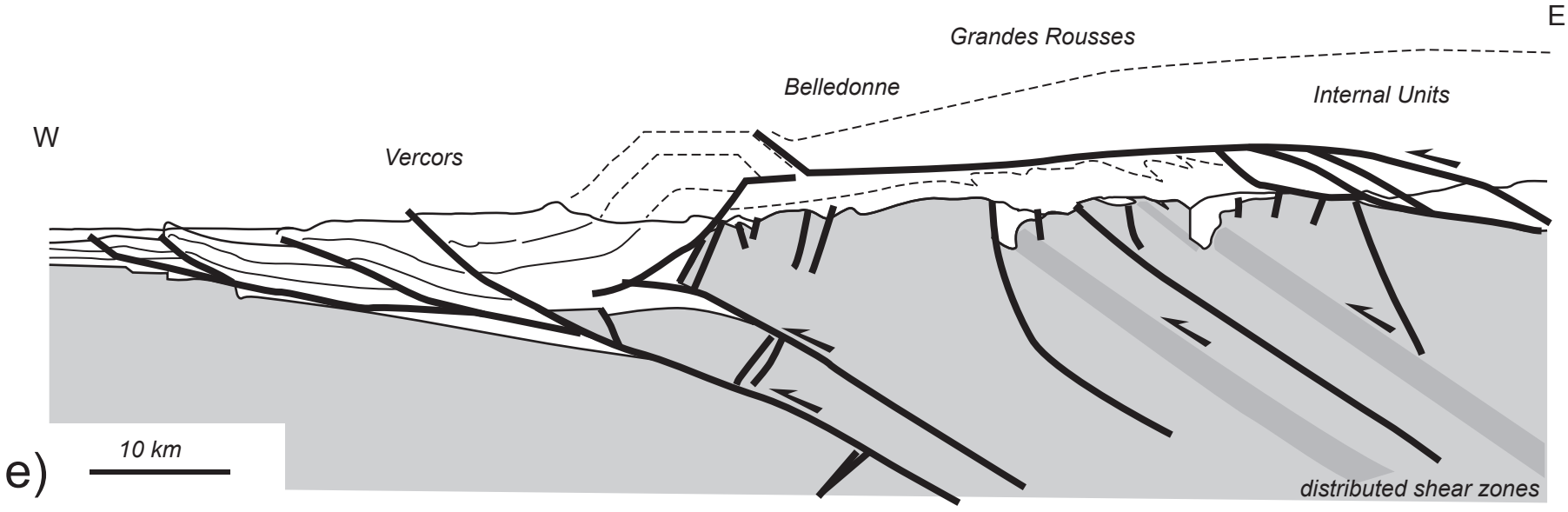

e)

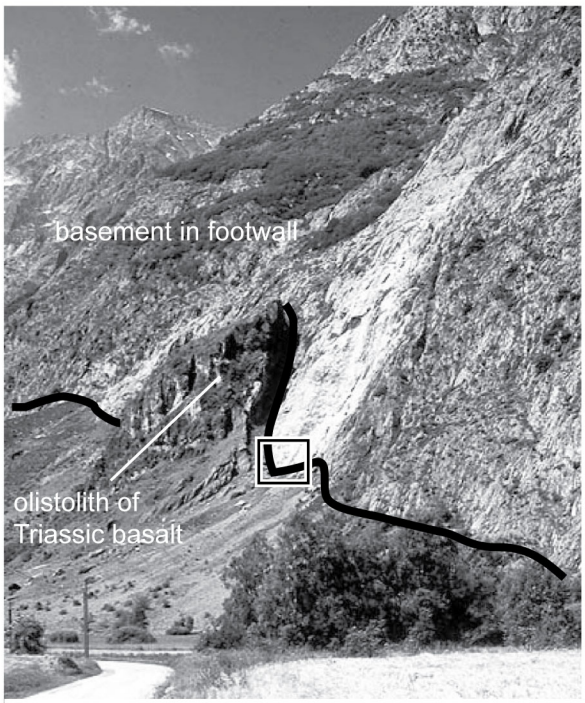
basement in footwall
olistolith of
Triassic basalt

a)

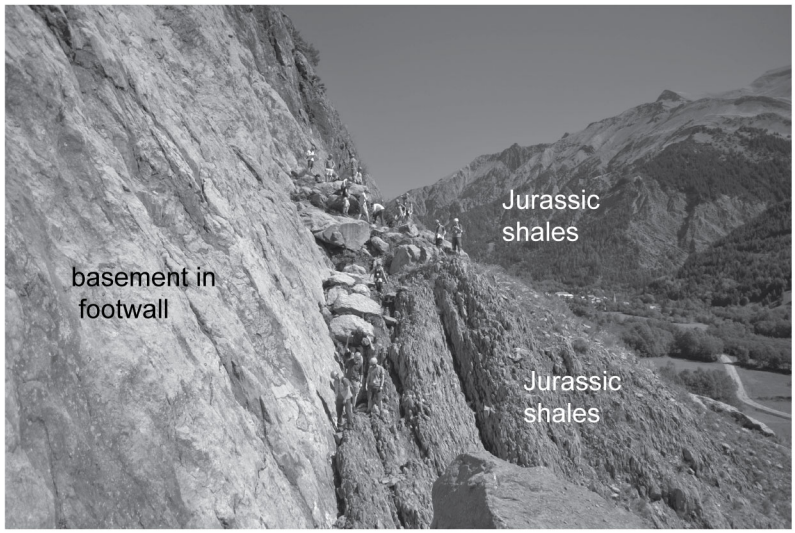
basement in
footwall
Jurassic
shales
Jurassic
shales

b)

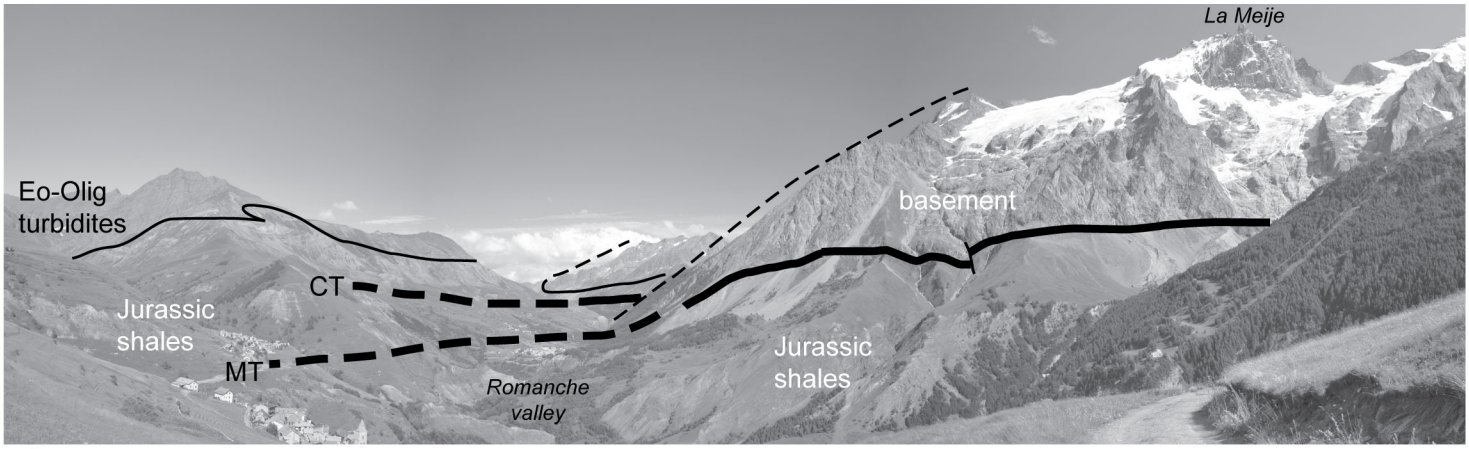
La Meije
Eo-Olig
turbidites
basement
CT
Jurassic
shales
MT
Romanche
valley
Jurassic
shales

c)

Figure 5

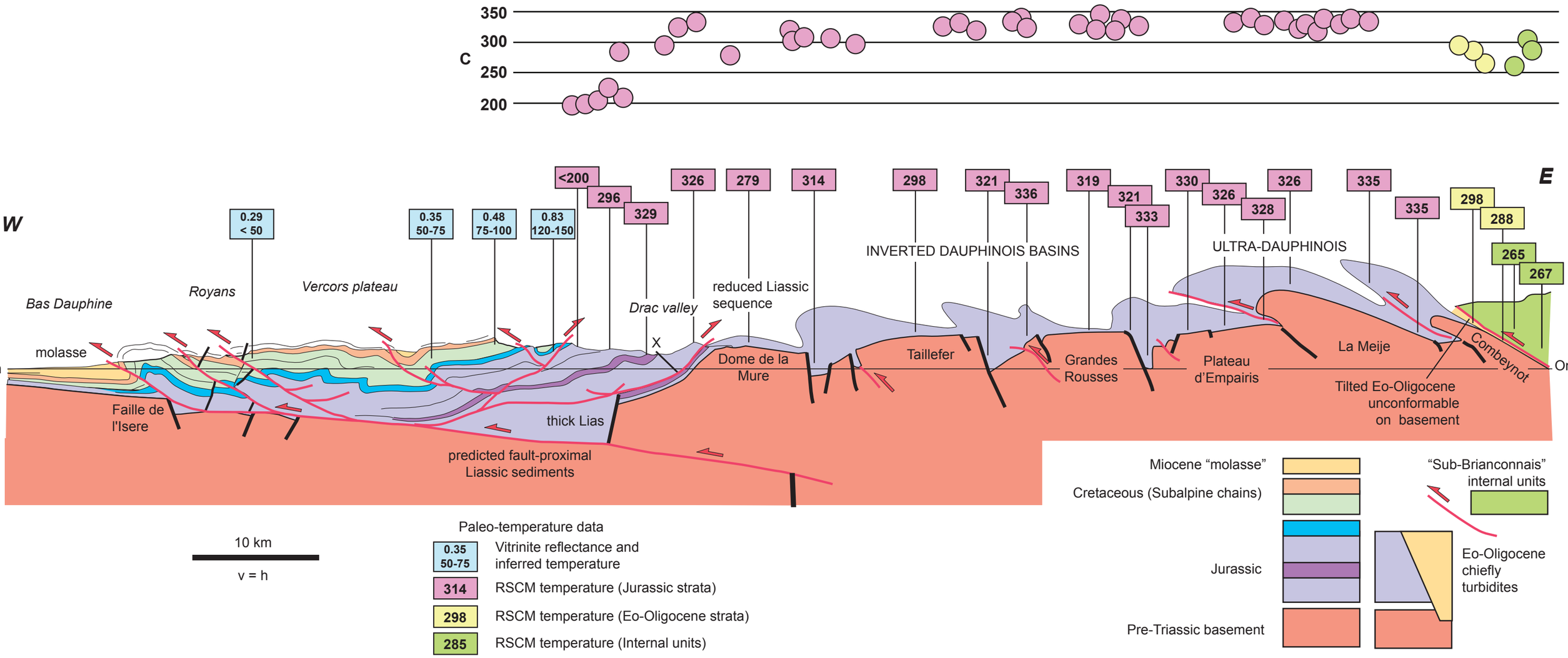
C
350
300
250
200
W
E
0.29
< 50
0.35
50-75
0.48
75-100
0.83
120-150
<200
296
329
326
279
314
298
321
336
319
321
333
330
326
328
326
335
335
298
288
265
267
Bas Dauphine
Royans
Vercors plateau
Drac valley
reduced Liassic
sequence
INVERTED DAUPHINOIS BASINS
ULTRA-DAUPHINOIS
molasse
Om
Faille de
l'Isere
thick Lias
predicted fault-proximal
Liassic sediments
Dome de la
Mure
Taillefer
Grandes
Rousses
Plateau
d'Empairis
La Meije
Combeynot
Tilted Eo-Oligocene
unconformable
on basement
10 km
v = h
Paleo-temperature data
0.35
50-75
Vitrinite reflectance and
inferred temperature
314
RSCM temperature (Jurassic strata)
298
RSCM temperature (Eo-Oligocene strata)
285
RSCM temperature (Internal units)
Miocene “molasse”
Cretaceous (Subalpine chains)
Jurassic
Pre-Triassic basement
“Sub-Brianconnais”
internal units
Eo-Oligocene
chiefly
turbidites

Figure 6

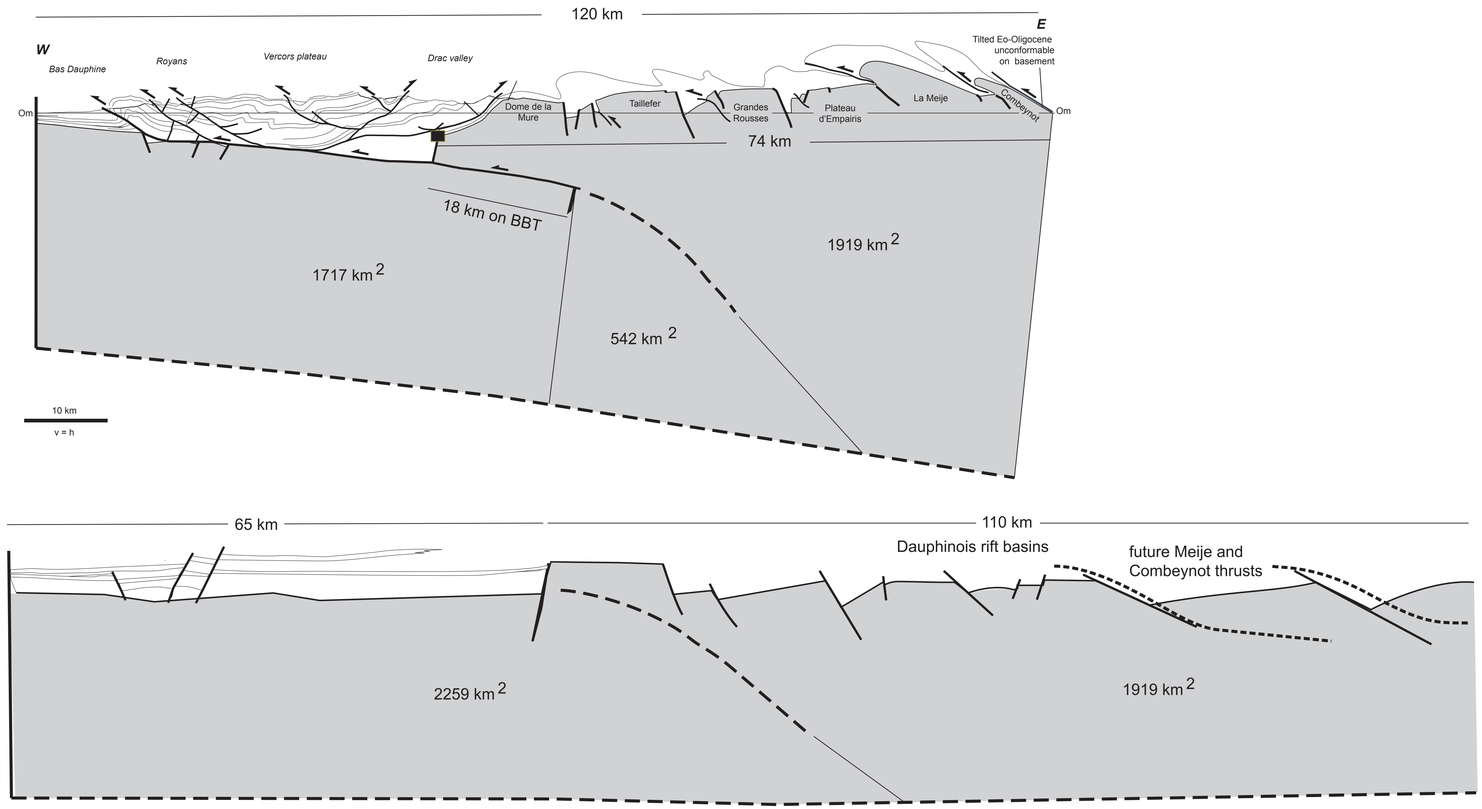
120 km
W
E
Bas Dauphine
Royans
Vercors plateau
Drac valley
Tilted Eo-Oligocene
unconformable
on basement
Om
Dome de la
Mure
Taillefer
Grandes
Rousses
Plateau
d'Empairis
La Meije
Combeynot
Om
74 km
18 km on BBT
1717 km 2
1919 km 2
542 km 2
10 km
v = h
65 km
110 km
Dauphinois rift basins
future Meije and
Combeynot thrusts
2259 km 2
1919 km 2

Figure 7

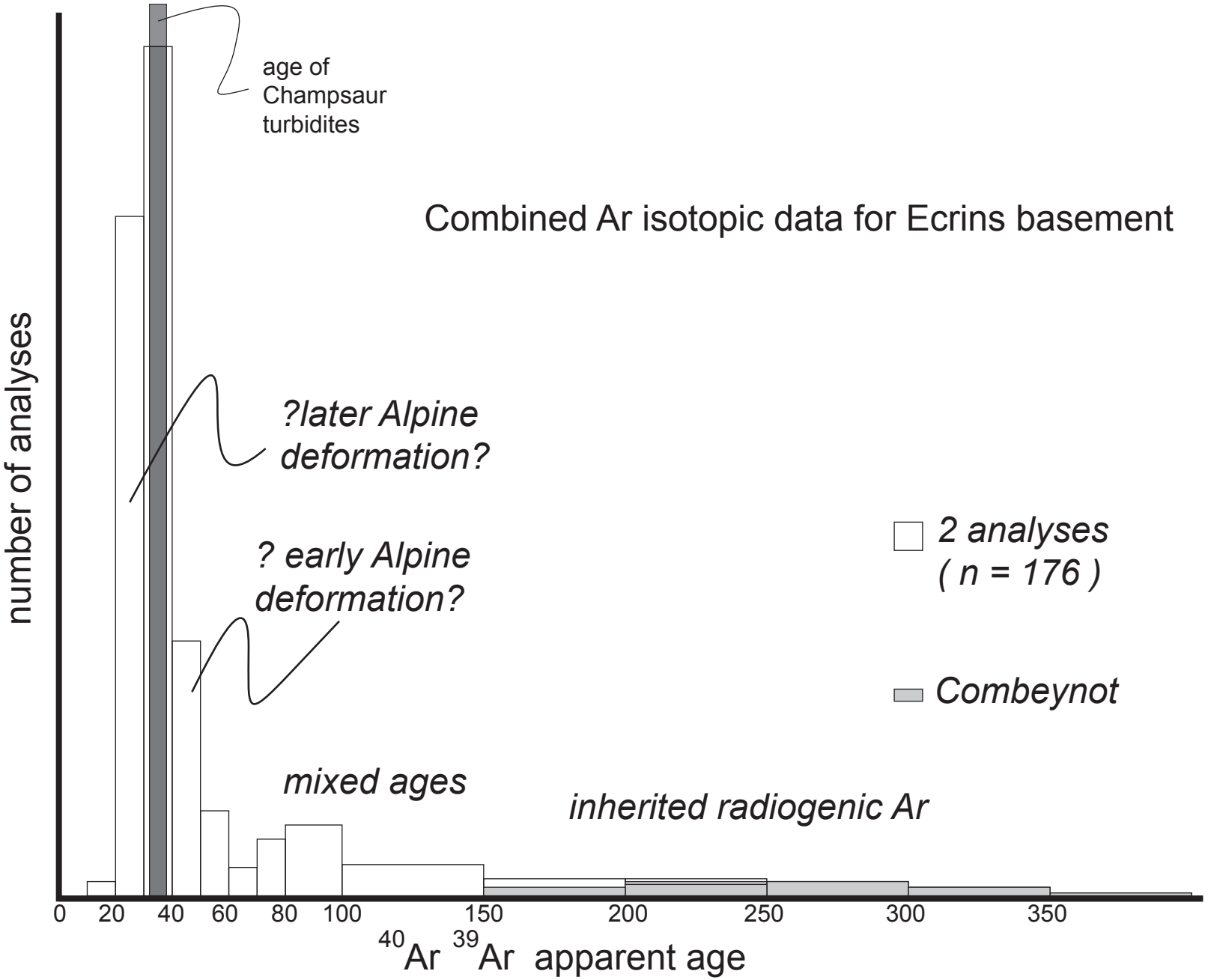
age of
Champsaur
turbidites
Combined Ar isotopic data for Ecrins basement
number of analyses
?later Alpine
deformation?
? early Alpine
deformation?
2 analyses
(n = 176)
Combeynot
mixed ages
inherited radiogenic Ar
0
20
40
60
80
100
150
200
250
300
350
40Ar 39Ar apparent age

Figure 8

Figure 9

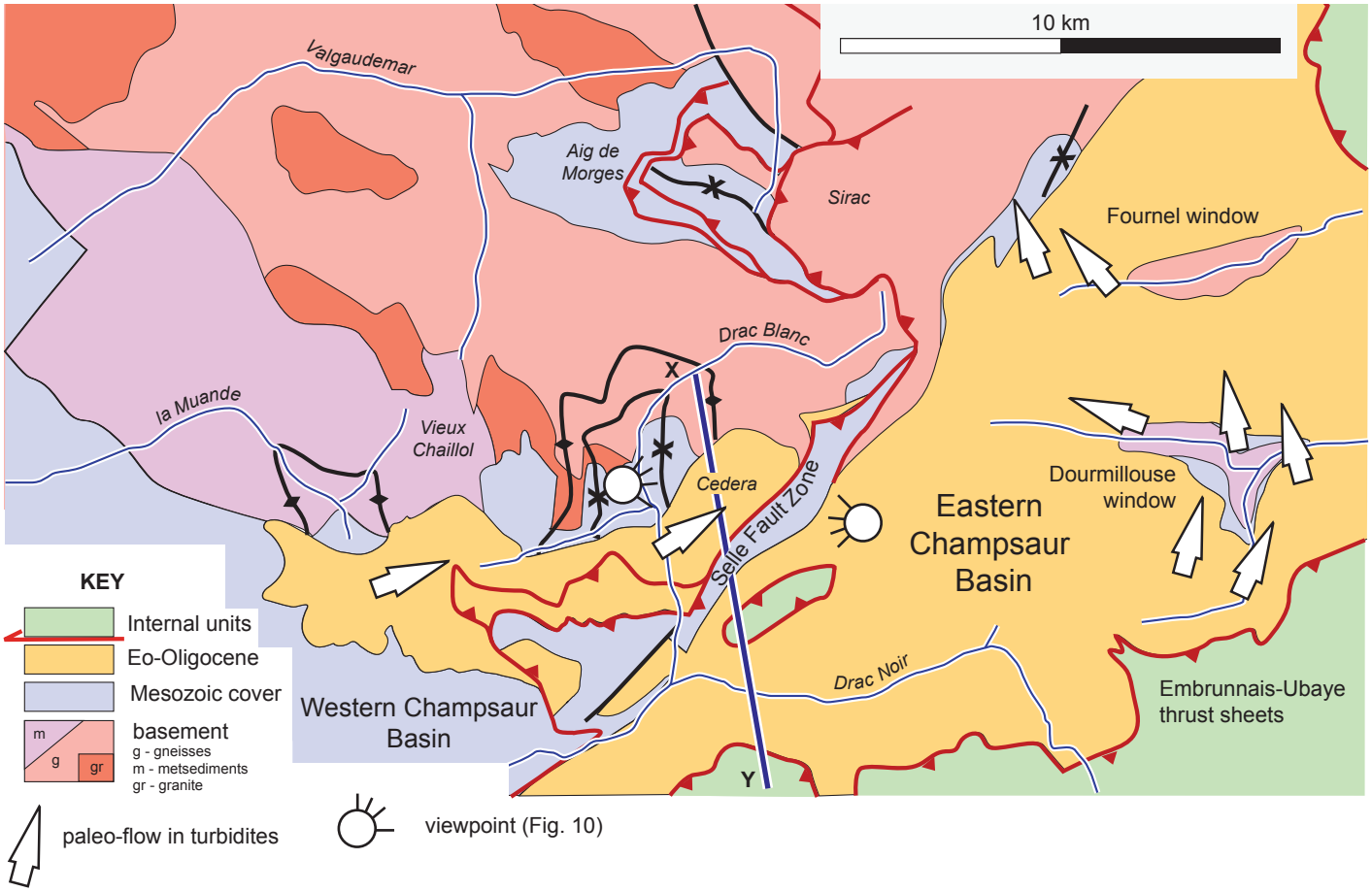
10 km
Valgaudemar
Aig de Morges
Sirac
Fournel window
Drac Blanc
X
la Muande
Vieux Chaillol
Cedera
Selle Fault Zone
Eastern Champsaur Basin
Dourmillouse window
Drac Noir
Western Champsaur Basin
Embrunnais-Ubaye thrust sheets
Y
KEY
Internal units
Eo-Oligocene
Mesozoic cover
basement
m
g
gr
g - gneisses
m - metsediments
gr - granite
paleo-flow in turbidites
viewpoint (Fig. 10)

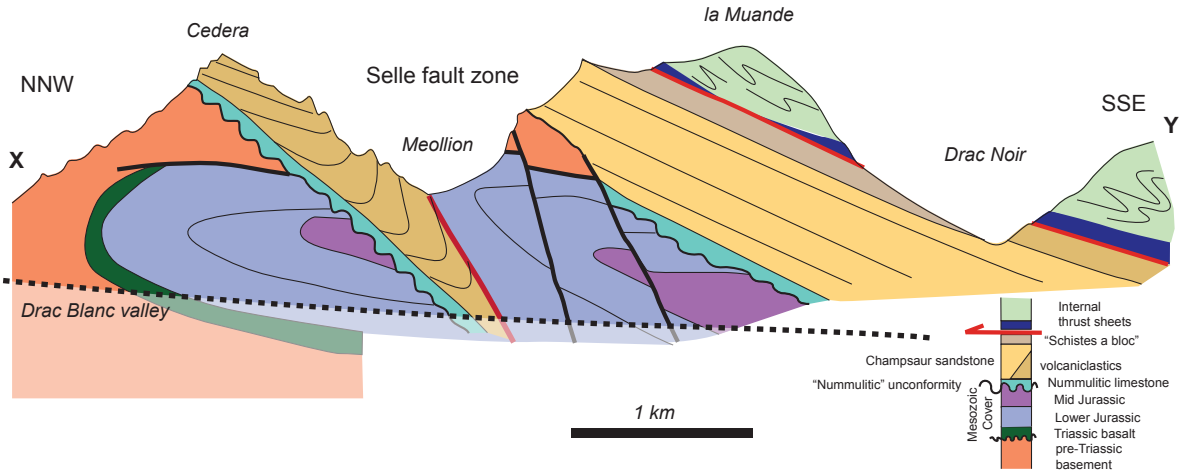
Cedera
la Muande
NNW
Selle fault zone
SSE
X
Meollion
Drac Noir
Y
Drac Blanc valley
1 km
Internal thrust sheets
"Schistes a bloc"
Champsaur sandstone
volcaniclastics
"Nummulitic" unconformity
Nummulitic limestone
Mesozoic Cover
Mid Jurassic
Lower Jurassic
Triassic basalt
pre-Triassic basement

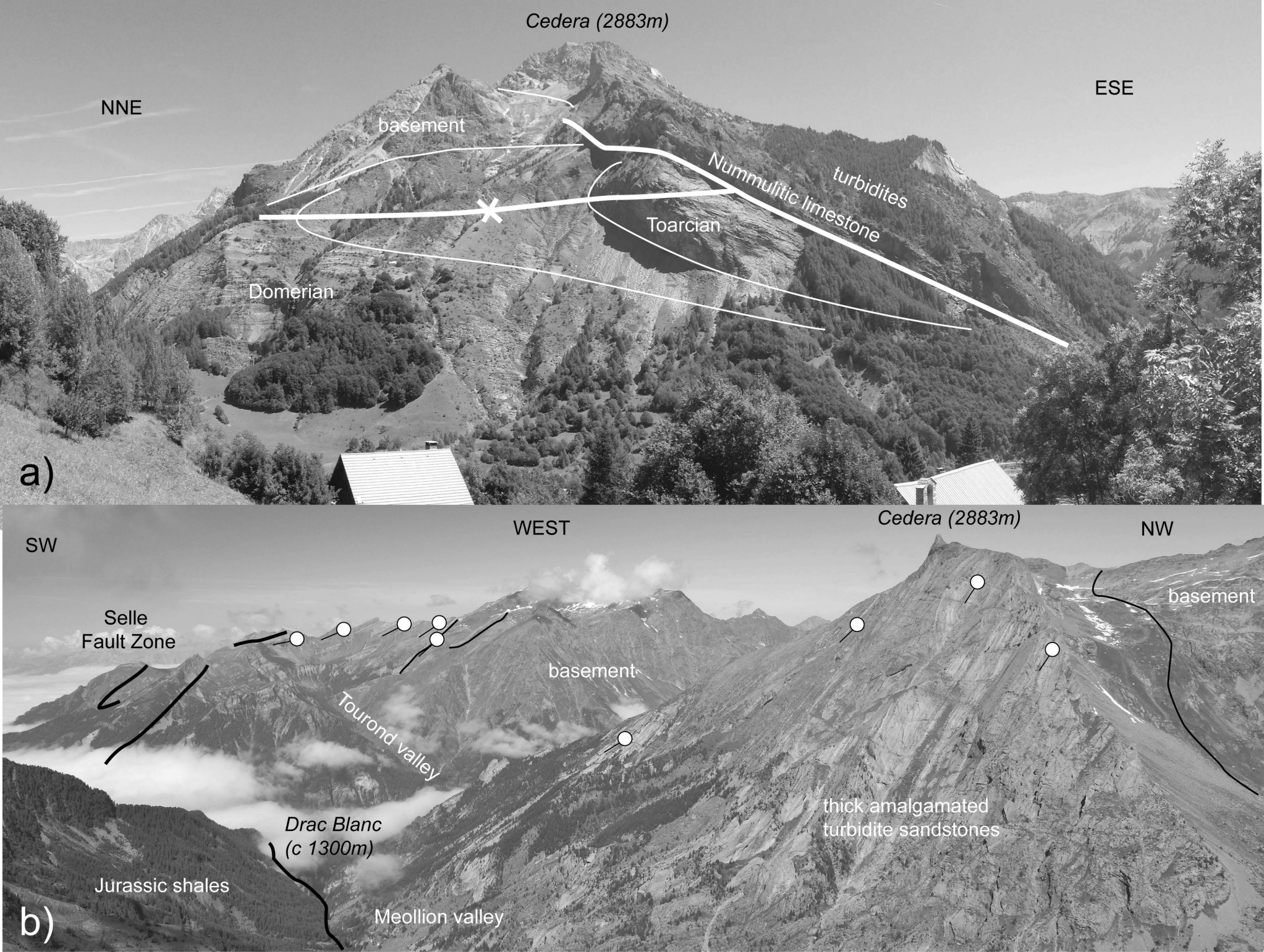
Cedera (2883m)
NNE
ESE
basement
Nummulitic limestone
turbidites
Toarcian
Domerian
a)
WEST
Cedera (2883m)
SW
NW
basement
Selle
Fault Zone
basement
Tourond valley
Drac Blanc
(c 1300m)
thick amalgamated
turbidite sandstones
Jurassic shales
Meollion valley
b)

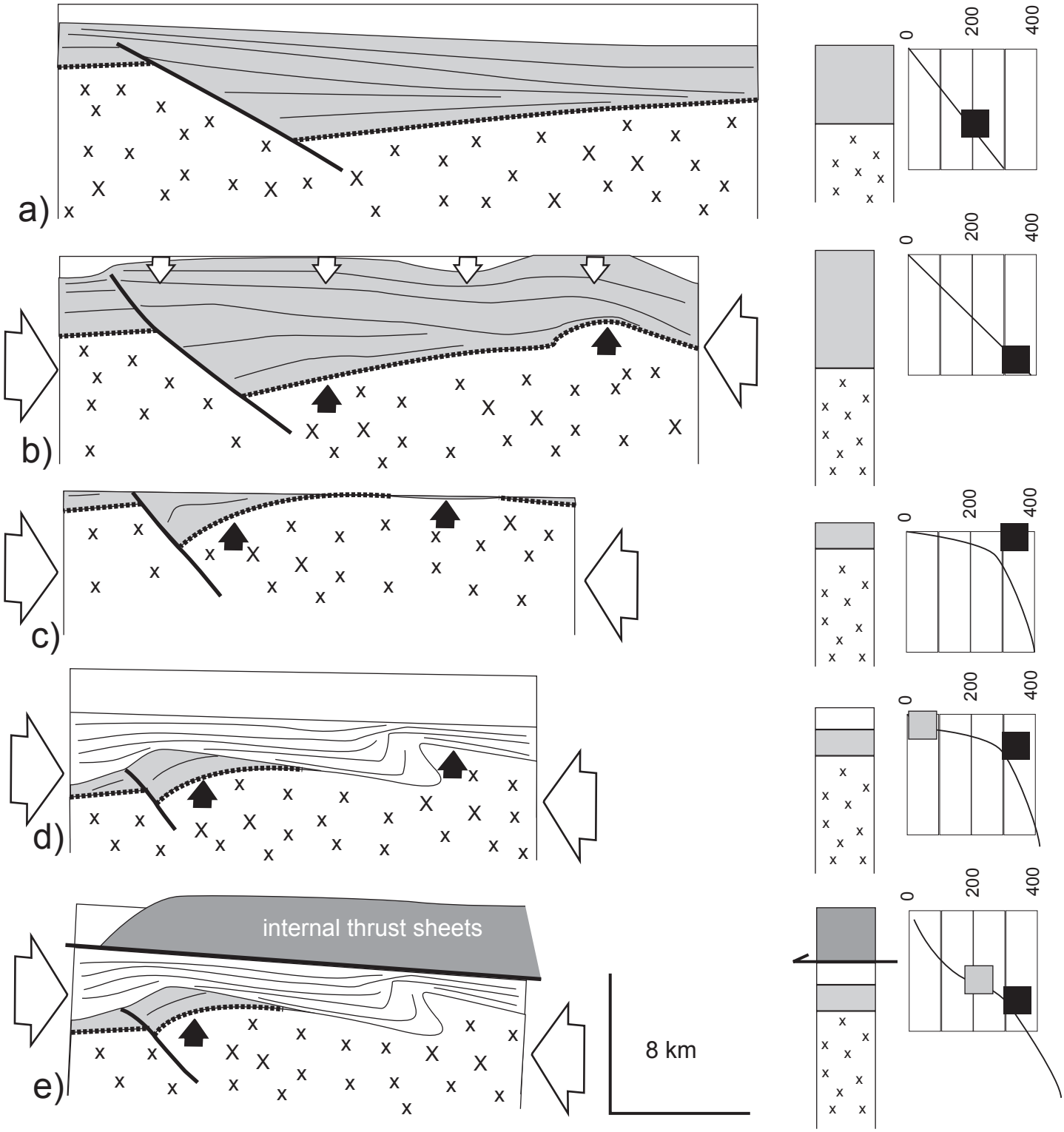

Figure 11

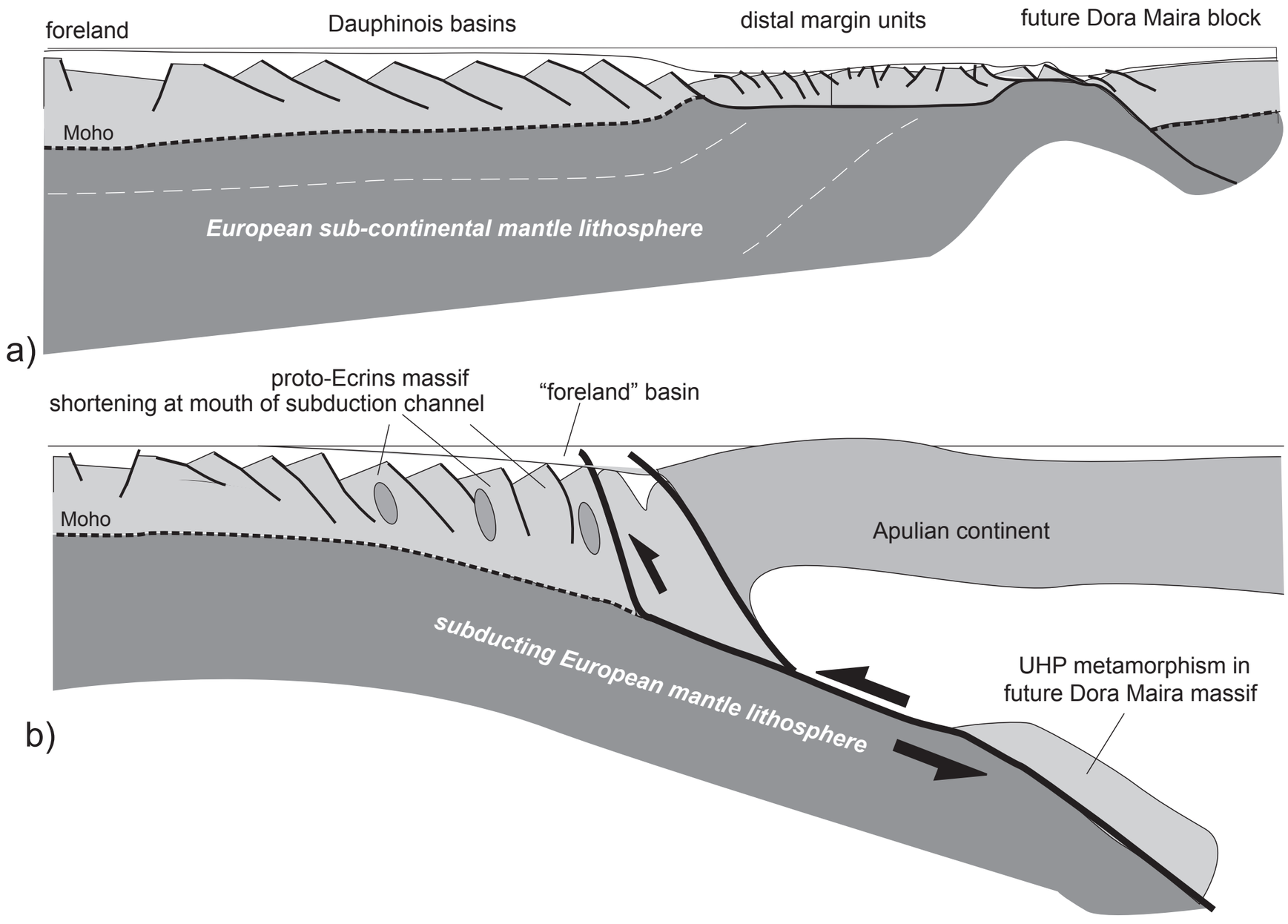

Butler
Figure 12